Eindhoven University of Technology

BACHELOR

Spatiotemporal characterization of dust-forming acytelene plasmas

Brooimans, R.J.C.

Award date:
2014

Link to publication

Spatiotemporal characterization of dust-forming acytelene plasmas

R.J.C. Brooimans

February 11, 2014   EPG 14-02

TU/e Supervisor: F.M.J.H. van de Wetering
Co-Supervisors: S. Nijdam, J. Beckers & G.M.W. Kroesen
Elementary Processes in Gas discharges
Eindhoven University of Technology

Abstract

In the plasma used for the experiments, dust particles spontaneously form under certain conditions. The whole process occurs in a matter of seconds to minutes after igniting the plasma and results in a cloud of particulates up to micrometer sizes levitated in the plasma. We studied a capacitively coupled radio-frequency plasma with constant flow of argon and acetylene (C_2H_2). After the dust cloud has been formed, an ellipsoid-shaped dust-free zone termed the void develops. Concurrently, the dust particles grow in size. During the void's expansion it suddenly stops growing and even shrinks, to shortly thereafter resume its expansion which we refer to as the hiccup. We infer this is induced by coagulation of a new batch of dust particles inside the void. The processes are periodical and reproducible. Measurements of the electron density of the plasma took place, accompanied by laser light scattering and emission spectroscopy.

One way to investigate the behavior of the void is to make use of the MCRS (Microwave cavity resonance spectroscopy) technique. In this research an aluminum cavity is used as a microwave resonance cavity. The cavity also serves as the discharge chamber. By sending out microwaves by an antenna, standing electric field waves inside the cavity can occur. Some microwave frequencies excite standing waves at which the cavity serves as a resonator. It seemed that a rather big cavity has a lot of resonant modes. Another reason why the cavity has a lot of resonant modes is because the cavity is surrounded by a metal mesh. In this research it is shown that replacing the mesh by solid aluminum reduces the amount of resonant peaks between 7-8 GHz. This way the quality of the cavity is improved.

The MCRS technique is used to link a measured resonant mode to a theoretical mode. These measurements took place in vacuum. This is done by using a dielectric to locally disturb the electric field inside the cavity. Due to this, the resonance frequency will shift. The magnitude of the resonance frequency's shift is a measure for the electric field at the position of the dielectric. By moving the dielectric, the electric field of a certain resonant mode can be determined. Due to this technique, the resonance frequency which is measured at 6.17 GHz, is believed to correspond to TM_{412}, where 4, 1 and 2 are indices for a specific mode. A second resonance peak was examined using the technique involving the dielectric. Because the measurements only took place in the xy-plane at $x = 0$, a one-to-one coupling between this mode and a theoretical mode could not be found. The coupling had a limitation, namely only measuring at $x = 0$. By moving the PVC cube in more directions, the coupling of the measured mode to a theoretical mode would become easier.

The MCRS technique is also used to measure the electron density of the plasma. During these measurements, some peculiar effects arose. The dust particles, when they enter the coagulation phase, start acting as an electron sink. Therefore, at the beginning, the electron density quickly rises where after it drops until it reaches an equilibrium. When these dust particles suddenly leave the discharge chamber because they become too large, the electron sink is gone. The plasma will react by temporarily increasing the electron density. This is shown by small bumps in the electron density graph.

The emission of the plasma was also measured, without using MCRS. The emission graph shows sharp periodical increases. The hypotheses for this effect is a new coagulation phase occuring inside the void. The inserted precursor molecules and/or radicals are efficiently adsorbed on the dust particles in the dusty region. In the void there are no dust particles so the inserted precursor molecules and/or radicals can and will start a new growth phase inside the void. Once this new growth cycle reaches the coagulation phase, the electron density will go down. Due to this decrease, the electron temperature will go up. The plasma will emit more photons if the argon line in question (in this research 763.51 nm) is particularly sensitive to electron temperature changes. Because an increase in emission is measured, it is clear that the argon emission line at 763.51 nm is sensitive to fluctuations in the electron temperature.

Contents

Chapter 1

Introduction

1.1 Dusty plasmas

A dusty plasma, or sometimes called complex plasma, is a plasma which contains nanometer- to micrometer-sized solid particles [1]. Whereas a pristine plasma containing ions, electrons and neutrals is already quite complex, the solid particles in a dusty plasma make it even more complex. Some phenomena in space science were indescribable using classic plasma physics. A huge part of space is, in fact, a dusty plasma. That was one of the main reasons why dusty plasma physics became an upcoming research field. A specific phenomenon that could not be described by the already known physics laws were the radial beams of the rings of Saturn [1]. Another example is the occurrence of dusty plasmas in deposition/processing plasmas. Especially these two examples were essential to the rise of dusty plasma physics. Some other examples of dusty plasmas in space are interplanetary dust, tails of comets and the Earth's (upper) atmosphere [1].

1.2 Goals and research questions

One of the goals in this research is to measure the electron density of the plasma. To determine the electron density of the plasma, microwave cavity resonance spectroscopy (MCRS) (see section 2.2.2 and 2.2.3) is used. Another technique to measure the electron density of a plasma involves Langmuir probes. Langmuir probes are not suitable for this research because of charged dust particles. Langmuir probes use electrons to measure the current, but because the dust particles are also negatively charged it is hard to study the behavior of the plasma using a Langmuir probe. That's why, in this research, MCRS is chosen. Some microwave frequencies excite a standing wave of the electric field inside the cavity. The associated three-dimensional electric field pattern can be calculated for an ideal cylindrical cavity and depends on the specific excited resonant mode. In a measured spectrum (see figure 4.1 on page 14) there are a lot of resonant modes visible. Due to this, and the imperfections in the cavity, coupling a measured microwave resonance peak to an ideal resonant mode is a challenge. Therefore, the main research goal is:

Determining the spatial electric field profile of a resonant mode which is used to measure the electron density.

These measurements took place in vacuum. The dusty plasma consists of an argon plasma containing dust particles. Although a chemical measurement of the dust particles has never been done, it is assumed the dust particles are C_2H_2 particles. Measurements of the dusty plasmas in this research involved emission of the plasma, scattering by the dust particles and the electron density of the plasma. Therefore, the second research goal is:

Determining the electron density of the Argon plasma containing dust particles, combined with the emission of the plasma and the scattering by the dust particles.

Chapter 2

Theory

2.1 Dust particles

In this research, a capacitively coupled radio-frequency plasma with a constant flow of argon and acetylene (C_2H_2) is studied. After igniting the plasma, the plasma is filled with particles up to micrometer sizes levitating in the plasma [1]. After the dust cloud has been formed, an ellipsoid-shaped dust-free zone develops. This dust-free zone is now referred to as the void [1]. After this, the dust particles grow in size. During the void's expansion it suddenly stops growing and even shrinks, to shorty thereafter resume its expansion which is from now-on referred as the hiccup. This hiccup is an important observation and will be used later in this report. The hiccup is caused by coagulation of a new batch of dust particles inside the void. This whole process is periodical and reproducible.

The growth of the dust particles inside the plasma is described in figure 2.1 on the next page. The stages are:

I. Formation of primary clusters: After the acytelene (C_2H_2) is inserted in the plasma, the acytelene molecules can polymerize due to the free electrons inside the plasma. The free electrons are generated by the plasma itself:

$$Ar + e^- \rightarrow Ar^+ + 2e^-. \tag{2.1}$$

The polymerization reactions are given by [3]

$$C_2H_2 + e^- \rightarrow C_2H^- + H, \tag{2.2}$$
$$C_2H^- + C_2H_2 \rightarrow C_4H_2^- + H. \tag{2.3}$$

The generalized polymerization reaction that takes place is given by [3]

$$C_{2n}H^- + C_2H_2 \rightarrow C_{2n+2}H_2 + H. \tag{2.4}$$

In equation (2.4), n is a positive integer.

II. Nucleation and cluster growth: The polymerized clusters grown in phase **I** can stick together. The sticking will happen at a certain critical radius (r_{crit}) where the dust particles transit from the gas phase to the solid phase. This is called nucleation.

III. Coagulation: Before coagulation, clusters are mainly neutral charged or single charged. The coagulation occurs for many particles at once. After the coagulation the dust particles act as tiny plasma 'probes' due to their (relative) large size. Therefore they act as a sink for electrons. At this stage the electron density inside the plasma will drop.

IV. Growth: The dust particles continue to grow in size by accretion of plasma ions and radicals. When the dust particles in this stage suddenly leave the discharge chamber, this sink of free electrons decreases in strength. During the plasma's response to this new situation, the electron density will temporarily go up, until ionization is at an equilibrium value again.
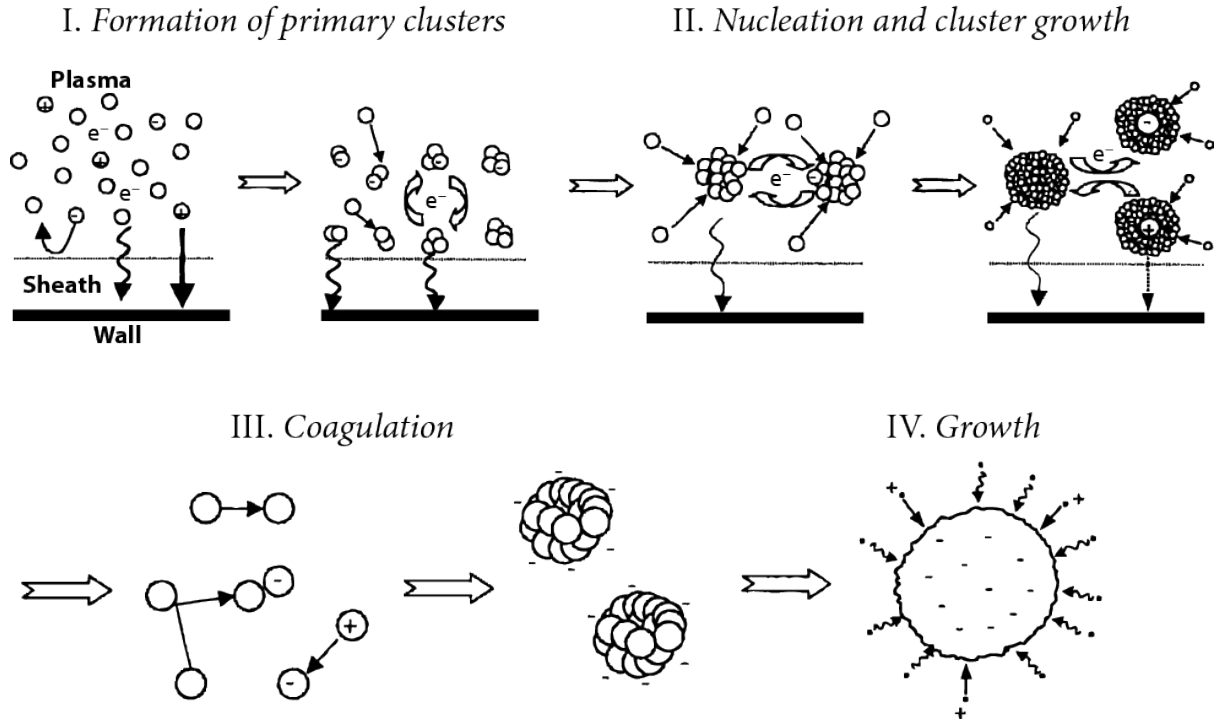
I. *Formation of primary clusters*   II. *Nucleation and cluster growth*

III. *Coagulation*   IV. *Growth*

Figure 2.1 – The growth of the dust particles inside the plasma.[2]

2.2 Microwave resonance

2.2.1 Geometry

In this research, an aluminum cavity is used as a microwave resonance cavity. The cavity is serves as the discharge chamber. The cavity is schematically shown in figure 2.2 on the following page.

There are two antennas in the cavity, see figure 3.2 on page 10. One antenna emits microwaves, the other serves as a detector. Two types of standing waves can occur in a closed cylindrical cavity: *transverse electric* (TE) and *transverse magnetic* (TM) modes. TE modes have no electric field in the direction of propagation, whereas TM modes have no magnetic field in the direction of propagation [4]. For a perfect cavity, the electric field patterns can be calculated. These equations are shown below [5].

General definitions:

$$k_3 \equiv \frac{p\pi}{d}, \tag{2.5}$$

$$k^2 \equiv k_1^2 + k_3^2. \tag{2.6}$$

$$E = \sqrt{E_r^2 + E_\phi^2 + E_z^2} \tag{2.7}$$

TM modes:

$$k_1 \equiv \frac{x_{mn}}{R}, \tag{2.8}$$

$$E_0 \equiv \sqrt{\frac{\mu}{\epsilon}} \frac{k_1}{k}, \tag{2.9}$$

$$E_r = -\frac{k_3}{k_1} E_0 J'_m(k_1 r) \cos(m\phi) \sin(k_3 z), \tag{2.10}$$

$$E_\phi = \frac{mk_3}{k_1} E_0 \frac{J_m(k_1 r)}{k_1 r} \sin(m\phi) \sin(k_3 z), \tag{2.11}$$

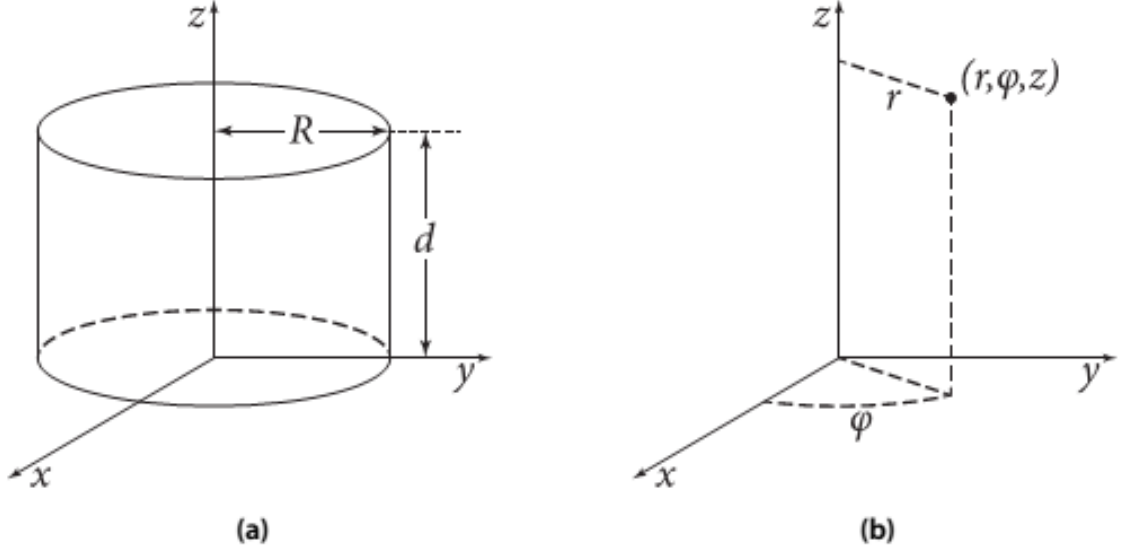$$E_z = E_0 J_m(k_1 r) \cos(m\phi) \cos(k_3 z). \tag{2.12}$$

3

Figure 2.2 – Schematic overview of the cavity. In (a) the parameters are shown, (b) are the regular cylindrical coordinates [1].

TE modes:

$$k_1 \equiv \frac{x'_{mn}}{R}, \tag{2.13}$$

$$E_0 \equiv -\sqrt{\frac{\mu}{\epsilon}}, \tag{2.14}$$

$$E_r = E_0 m \frac{J_m(k_1 r)}{k_1 r} \sin(m\phi) \sin(k_3 z), \tag{2.15}$$

$$E_\phi = E_0 J'_m(k_1 r) \cos(m\phi) \sin(k_3 z), \tag{2.16}$$

$$E_z = 0. \tag{2.17}$$

In equations (2.5) to (2.17), m is the order of x_{mn}, the nth root of the equation $J_m(\zeta) = 0$. There are three indices, namely m, n and p, because the cavity is three-dimensional. The indices m, n and p are discrete and can have the following values [5]:

$$m = 0, 1, 2, ...$$
$$n = 1, 2, 3, ...$$
$$p = 0, 1, 2, ...$$

For the TE modes,

$$p = 1, 2, 3, ...$$

In equations (2.5) to (2.17), μ is the magnetic permeability of the medium inside the cavity and ϵ is the absolute permittivity of the medium inside. When $\mu = \mu_0$ and $\epsilon = \epsilon_0$, the resonance frequencies in vacuum are calculated and $\frac{1}{\sqrt{\mu_0 \epsilon_0}}$ reduces to the speed of light c. When the cavity is filled with a medium, $\mu \neq \mu_0$ and $\epsilon \neq \epsilon_0$, the resonance frequency will shift. Furthermore, μ is always assumed to be μ_0. A certain TM/TE mode is now referred to as TM$_{mnp}$/TE$_{mnp}$. $J_m(\zeta)$ is a solution of the (Bessel) differential equation given by [6]

$$\zeta^2 \frac{\mathrm{d}^2 y}{\mathrm{d}\zeta^2} + \zeta \frac{\mathrm{d}y}{\mathrm{d}\zeta} + (\zeta^2 - m^2)y = 0. \tag{2.18}$$

For both TM and TE, the resonance frequencies can be calculated. They are given by [5]

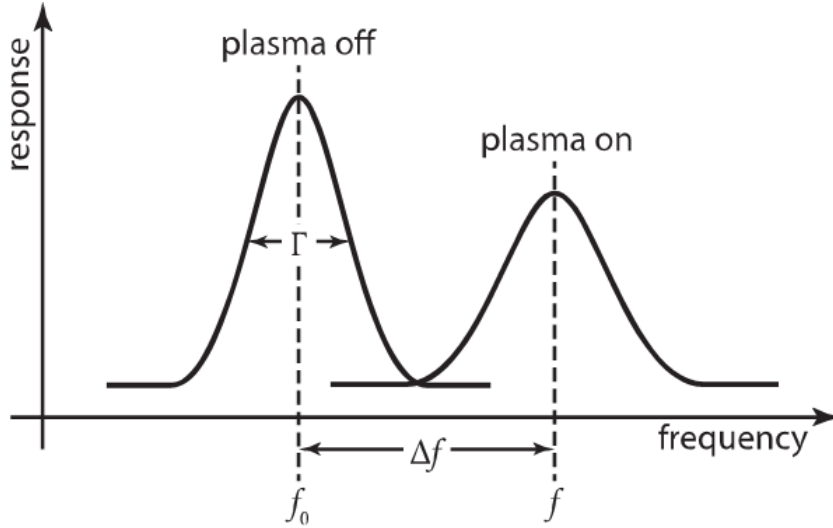$$f = \frac{k}{2\pi\sqrt{\mu\epsilon}}. \tag{2.19}$$

4

Figure 2.3 – The resonance frequency will shift when the plasma is turned on.[1]

2.2.2 Electron density

When the cavity is in vacuum, certain microwave frequencies will show a response on the detecting antenna. Specific microwave frequencies will excite resonant modes in the cavity. At resonance this signal is maximal. Once the plasma is turned on, this resonance peak will shift due to a change in medium permittivity, caused by a change in electron density. Figure 2.3 shows what will happen.

When there is no plasma, only free electrons naturally present in a lab environment will contribute to the electron density. This density is orders of magnitude lower than the electron density of a plasma. Therefore the free electron density is safely ignored. The electron density is given by [1]

$$\overline{n}_{\mathrm{e}} = \frac{8\pi^2 m_{\mathrm{e}} \epsilon_0 f^2}{e^2} \frac{\Delta f}{f_0}, \tag{2.20}$$

with $\overline{n}_{\mathrm{e}}$ the *averaged* electron density, m_{e} the (rest) mass of an electron, ϵ_0 the electric permittivity of vacuum, Δf the frequency shift, f_0 the resonance frequency without the plasma turned on and f the resonance frequency when the plasma is turned on.

So, the resonance frequency shift will only determine the *averaged* electron density of the plasma. A space-resolved electron density distribution function can be retrieved from the following equation [1]:

$$\overline{n}_{\mathrm{e}} = \frac{\int\limits_{cavity} n_e(\vec{x}) E^2(\vec{x}) \mathrm{d}\vec{x}}{\int\limits_{cavity} E^2(\vec{x}) \mathrm{d}\vec{x}}. \tag{2.21}$$

The subscript "cavity" means that the volume integral is taken over the whole cavity. $\vec{x}$ is the point (x,y,z) in cartesian coordinates. $n_e(\vec{x})$ is the electric field and $E^2(\vec{x})$ is the square of the electric field magnitude at this point inside the cavity. It is essential to retrieve knowledge about $E(\vec{x})$ because it is a weighting factor for the electron density inside the cavity, see equation (2.21). When $E(\vec{x})$ is known, information about where changes in electron density have happened can be retrieved. This is only possible when more modes are combined but this is not trivial.

2.2.3 Dielectric

As shown in section 2.2.2, the electron density is space averaged and electric field weighted over the cavity. One way to determine $E(\vec{x})$ is to locally and systematically disturb the medium inside the cavity with a dielectric. This is done by using a PVC cube. Due to this changed electric field, the resonance frequency will shift. The magnitude of the frequency shift depends on the local value of E. They are correlated by [7]

5

$$\int\limits_{PVC\,Cube} E^2(\vec{x})d\vec{x} \propto \frac{f_0 - f}{f}. \tag{2.22}$$

As shown in equation (2.22), the local change in the electric field is correlated to the shift in the resonance frequency for a dielectric located at $\vec{x}$ in the cavity.. The higher the resonance frequency shift, the higher the electric field and thus weighting of the electron density is at the position where the dielectric PVC cube is located.

2.3   Scattering

For small dust particles, when $r_d \leq \frac{\lambda}{10}$ (r_d is the radius of the dust particles and λ the wavelength of the light), Rayleigh scattering describes the scattering by the dust particles [8]. When $r_d > \frac{\lambda}{10}$, Mie scattering describes the scattering by the dust particles [8]. In this research, nanometer to micrometer size particles have been used and the wavelength of the laser used is 532 nm. Therefore Mie scattering is used to describe the scattering by the dust particles.

The following equation holds for the scattering by the dust particles [8]:

$$\frac{\Phi_{\mathrm{s}}}{\Phi_0} = Gn_d \left(\frac{\lambda}{2\pi}\right)^2 \cdot f(m,\alpha,\gamma), \tag{2.23}$$

with Φ_{s} the scattered flux, Φ_0 the incident light flux, G a geometry coefficient related to how the experiment is set up, n_d the dust particle number density and λ the wavelength of incident light. In these experiments a 532 nm laser is used so $\lambda = 532$ nm. f is a complicated (mie) scattering function in which m is the complex refractive index of the dust particles, α a size parameter depending on the dust particle radius (r_d) and γ a geometry coefficient, just as G.
During one experiment some parameters remain constant. This is the case in the experiments described in this report. Equation (2.23) then reduces to:

$$\frac{\Phi_{\mathrm{s}}}{\Phi_0} \propto n_d \cdot f(m,\alpha,\gamma). \tag{2.24}$$

By placing a laser line filter (532 nm) in front of a camera the scattering by the dust particles can be recorded and the void can be visualized.

2.4   Emission

Emission in a plasma occurs when an electron bound to an atom or ion transits from a higher energy state to a lower energy state. In a plasma, an electron is excited to a higher energy state by impact of another electron or collisions between atoms/ions. The energy emitted of the photon when the electron returns to a lower energy state is equal to the difference between the energy of the two states.

A few possible transitions in argon are shown in figure 2.4 on the following page.

In this research the emission peak at 763.51 nm is used to measure the emission. It is highlighted in figure 2.4.
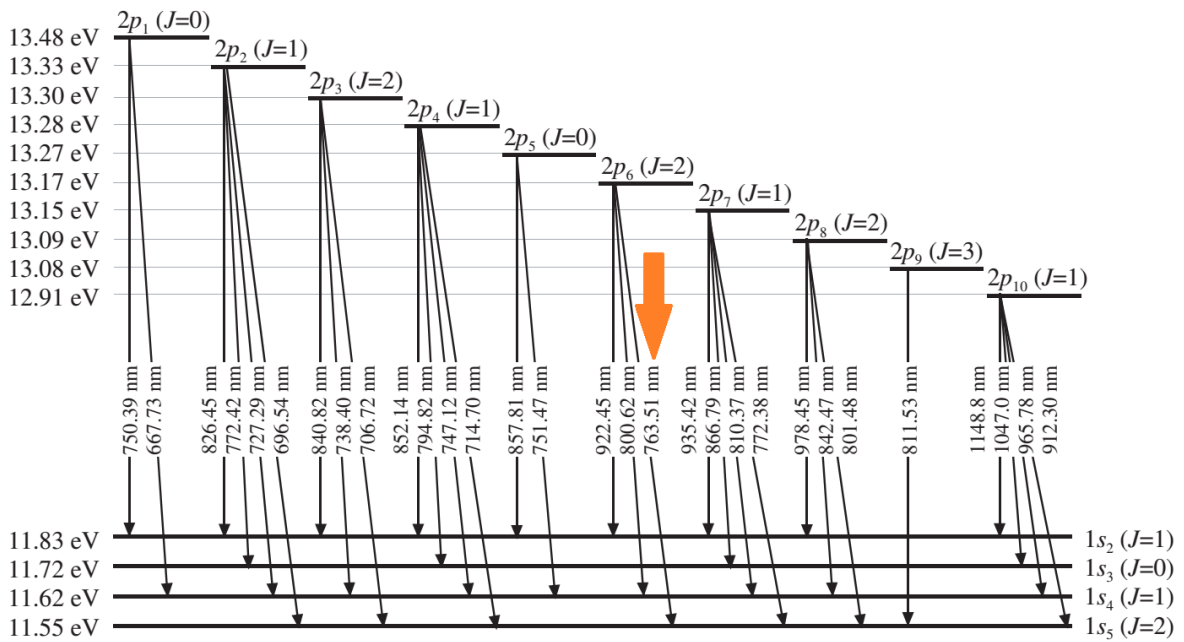
Figure 2.4 – The possible transitions in Argon and their corresponding energy differences and emitted wavelengths. The transition that emits light of 763.51 nm is highlighted in the figure and is used in this research.[9]

Chapter 3

Experimental setup and methods

3.1 Global setup

The global setup used for the measurements is schematically shown in figure 3.1 on the next page. It is divided into two parts. On the left a front view of the setup, which is used for the resonance and electron densities measurements, can be seen. On the right a top view of the setup, which is used for the emission and scattering experiments, can be seen.

The Ar/C_2H_2 flow is shown in orange. The gas is inserted from the top of the cavity. The Ar/C_2H_2 gas flow is inserted through a shower head. The gas then flows through small holes in an electrode, which also serves as the powered electrode for the plasma. The rest of the components in figure 3.1 are:

Laser, Thorlabs DJ532-10: The laser diode (532 nm) is used for the scattering experiments described in section 3.3.2. The laser is focused by lenses to create a 2D-plane. The first two lenses are used to collimate the laser beam to the right diameter. The third lens is a cylindrical lens to focus the laser light into a 2D-plane. The 2D laser plane can be used to scatter light on the dust particles.
Microwave generator, Giga-Tronics model 605: The microwave generator generates the microwaves which are emitted by the first antenna. The modulation frequency is determined by the function generator.
Function generator A, Agilent 33220A: The function generator provides the modulation input for the microwave generator. Some examples are a fixed frequency or a modulation of the frequency.
Function generator B, Agilent 33280A: The function generator provides the triggering of the DAC system to keep track of the timing of all experiments.
DAC, TU/e DACS: The DAC (Digital-to-Analog Converter) serves as an acquisition system and synchronizes the experiments. On top of that, the DAC system converts the binary numbers into physical quantities. In this case the DAC converts the binary number from the transducer into a voltage.
Transducer, Agilent 8472B Crystal Detector: The transducer is connected to the detector antenna. The signal that arrives at the detector antenna is an AC signal. The transducer converts this to a DC signal.
Amplifier, Amplifier Research Model 75A250: The power for the energy providing electrode is generated by a function generator which is set at 13.56 MHz alternating current. The voltage is too low to ignite the plasma, so the (RF) amplifier amplifies the power. The amplifier can amplify the signal up to 50 W.
Matchbox, in-house built: The impedance of the function generator which provides the power for the amplifier is set at 50 Ω. The matchbox matches the impedance of the amplifier to the impedance of the plasma, which is unknown, to maximize energy efficiency. If the impedances were not matched, too much power would be dissipated in the cables and the amplifier which may cause malfunctioning of the devices.
SmartPIM, Scientific Systems 0042501: The Smart PIM device measures several quantities inside the plasma. It is used to measure the power, voltage, current, impedance and the phase shift. The measured impedance of the plasma can be combined with the matchbox to maximize energy efficiency.
Beam splitter: The beam splitter splits the light from the cavity into two perpendicular paths having equal intensities. This way, 50% of the intensity of the light is recorded by the first CMOS and 50% of the intensity of the light is recorded by the second CMOS.
Pulse Generator, Tektronix CFG 250: The pulse generators generates 10 Hz pulses to synchronize
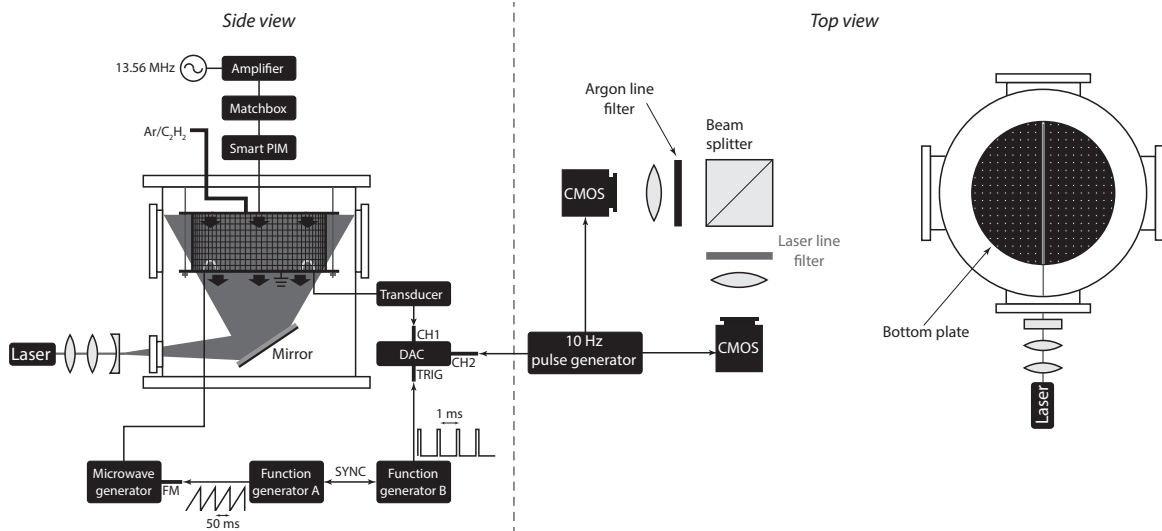
Figure 3.1 – The (schematical) global setup used for the experiments.

the cameras and the electron density signal.

CMOS, The Imaging Source DMK 23GM021: The two CMOS's are cameras. One camera measures the emission of the plasma while the other camera measures the scattering by the dust particles.

Laser line filter: This filter only transmits light at 532 nm. Its FWHM (Full Width at Half Maximum) is 10 nm. The laser emits light at 532 nm. This way the scattering by the dust particles inside the plasma is recorded by the CMOS behind the laser line filter.

Argon line filter, Thorlabs FB 760-10: The argon line filter transmits light of the emission peak at 763.51 nm. Its centre wavelength is 760 ± 2 nm. (see section 2.4). Its FWHM is 10 ± 2 nm. The emission line at 763.51 nm is the only peak inside the filter's range. See figure 3.5 on page 12 for the transmission wavelengths graph of the filter.

3.2 Microwave cavity resonance spectroscopy

As described in section 2.2.3, a dielectric PVC cube is used for these measurements. The setup is schematically shown in figure 3.2.

As can be seen in figure 3.2 on the next page, the antennas are now clearly visible in the cavity. There is also a thin nylon string located inside the cavity, to which the PVC cube is attached. The arrows show the directions in which the PVC cube is moved along the cavity.

To determine the resonance frequencies of the cavity, the following measurement technique is used. The microwave generator is set at a start frequency and an end frequency with a certain increment. To determine the whole spectrum from 2 GHz to 8 GHz, the increment was set at 1 MHz. Whenever zooms of the spectrum needed to be measured, the increment was changed to 500 kHz. This way, the total measurement time can be influenced. The transient recorder was set at 100 records per record, which is equal to 100 sample points per frequency (only one of these is used to obtain the spectrum). The time between two frequency measurements is about 100 ms. Each record is retrieved from the transducer, which measures the response of the detecting antenna. This results in a spectrum as shown in figure 4.1 on page 14.

To determine the electron density in a dusty plasma, the FM modulation method was used. First of all a frequency modulation of the microwave generator was used. A center frequency (f_c) and a modulation (ΔF) of about 10 MHz were applied to the microwave generator. The modulation applied is a sawtooth. The resulting output frequency is shown in figure 3.3 on the next page.

Function generator A (see section 3.1) responsible for this frequency modulation outputs a 20 Hz sawtooth (which corresponds to a period of 50 ms). Function generator B responsible for the actual data acquisition outputs trigger pulses at 1 kHz (1 ms). These function generators are coupled and synchronized, so they are in phase. In other words, function generator B triggers the sampling of the cavity response (the output of the transducer behind the receiving antenna). This way exactly 50 responses (voltages) are retrieved from the transducer during one cycle, t_m. The exact modulation
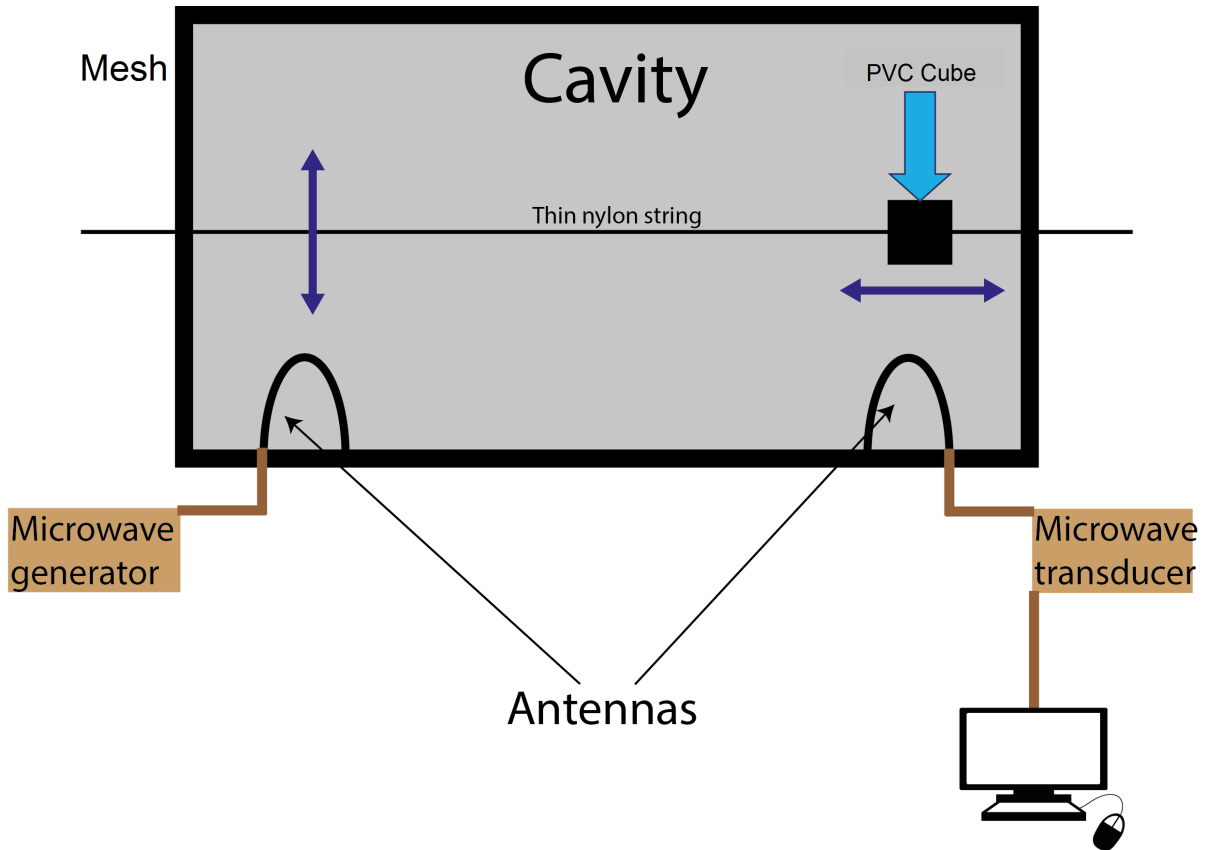
Figure 3.2 – Schematic side overview of the cavity. This is the setup used for microwave cavity resonance spectroscopy.

Figure 3.3 – The frequency as delivered by the microwave generator in time resulting from applying a sawtooth input signal. Each modulation cycle, shown by t_m, takes 50 ms. The sample time or measuring time shown by t_s is 1 ms. The green line indicates the center frequency f_c. The minimum frequency and maximum frequency of the modulation are shown as well.

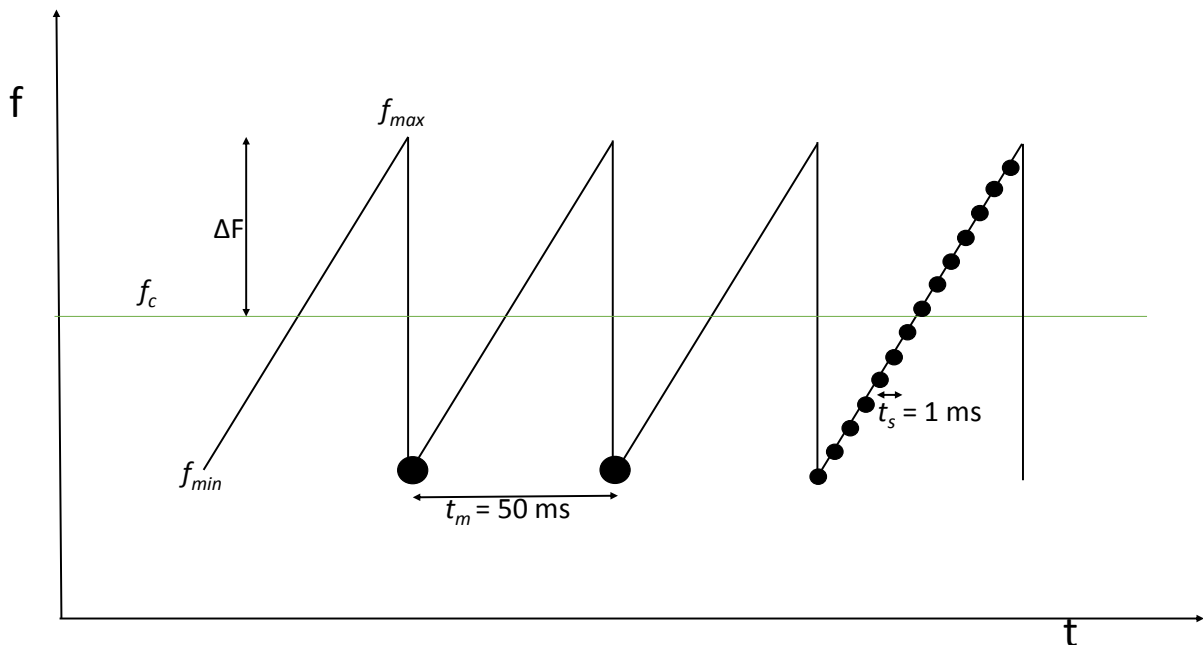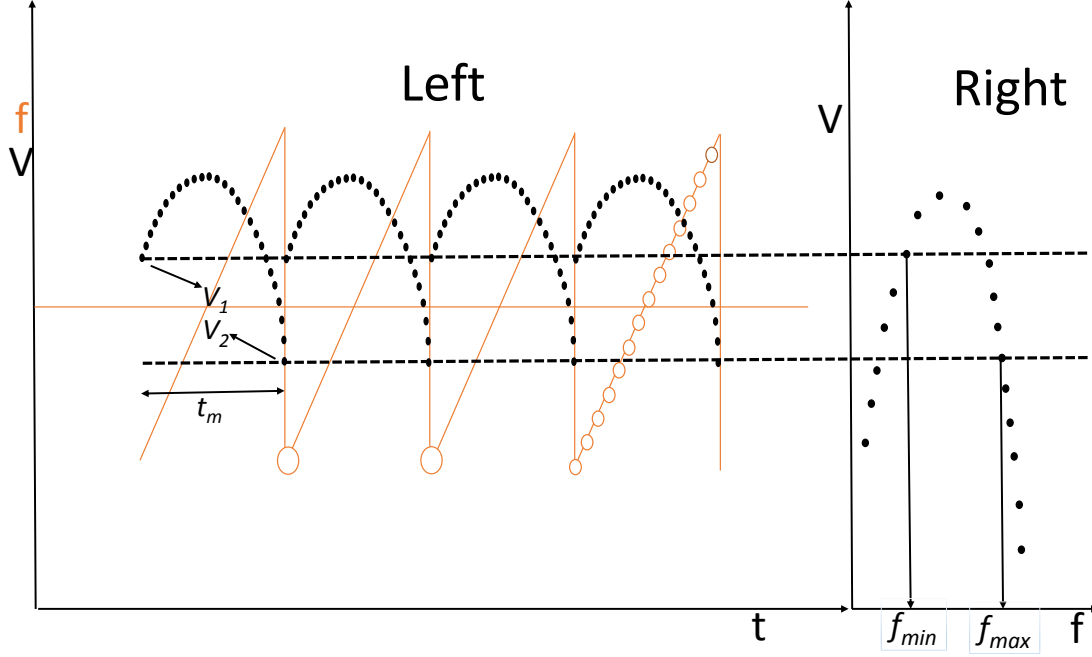**Figure 3.4** – Left: In black, a typical measurement done with the FM method. To correlate the figure to figure 3.3, figure 3.3 is shown in orange. One cycle corresponds to t_m, V_2 corresponds to f_{min} and V_2 corresponds to f_{max}. Right: The discrete output function of the microwave generator. A single resonance curve is obtained.

frequency ΔF is not known. That is why a calibration is necessary. Figure 3.4, in the left, shows a typical raw measurement.

The first sample recorded, shown by V_1, corresponds to $f_{\min}$ while the 50th sample, shown by V_2, corresponds to $f_{\max}$. However, it is not known what the exact values of $f_{\min}$ and $f_{\max}$ are (in Hz). To determine compare cavity responses in vacuum are compared, once using the FM modulation method and once using the conventional discrete output function of the microwave generator (for which the exact frequencies are known). So, several FM cycles are measured, producing an output analogous to the black dots in the left of figure 3.4. The mean value of V_1, as well as V_2, is determined over all cycles. Using the discrete output function of the microwave generator a single resonance curve is also obtained, this is shown in the right of figure 3.4. Here, for every measurement point both f and V are known. Since the conditions in vacuum are identical for both methods (FM and discrete), $f_{\min}$ and $f_{\max}$ follow from linking (interpolating) the cavity response voltages for both methods, see figure 3.4.

When the plasma is turned on, the FM method is used to measure over a long time. This way a lot of cycles shown in figure 3.4 are measured. By cutting these cycles into cycles of 50 samples, each modulation has its own data. For each cycle the resonance frequency can be determined through fitting using a fourier series with three components. The electron density follows from equation (2.20) and is therefore determined with 50 ms time resolution during a dusty plasma experiment.

3.3 Emission and scattering

For both the emission and the scattering experiments, a CMOS camera described in section 3.1 is used. They are triggered by the pulse generator at 10 Hz to synchronize the timing of the experiments. As a result, they record at 10 frames per second. The same triggering signal is sent to the acquisition system (DAC) for the electron density to synchronize.

3.3.1 Emission

The emission spectrum of the Ar/C_2H_2 plasma is measured using an Ocean Optics HR2000+ spectrometer. It is shown in blue in figure 3.5 on the next page.

To measure the emission of the plasma of the peak at 763.51 nm, a filter has to be used. The filter's (described in section 3.1) transmission is plotted in red in figure 3.5. It is clear that the peak at 763.51

nm is enclosed by the transmission of the argon line filter. Applying this filter will properly emit the light that is used for the emission measurements.

3.3.2 Scattering

The filter used for the scattering experiments transmits light at 532 nm. This way it only transmits the laser plane light which scatters the dust particles. Because there are no dust particles inside the void there will be no scattering inside the void. This way these experiments will clearly visualize the void.
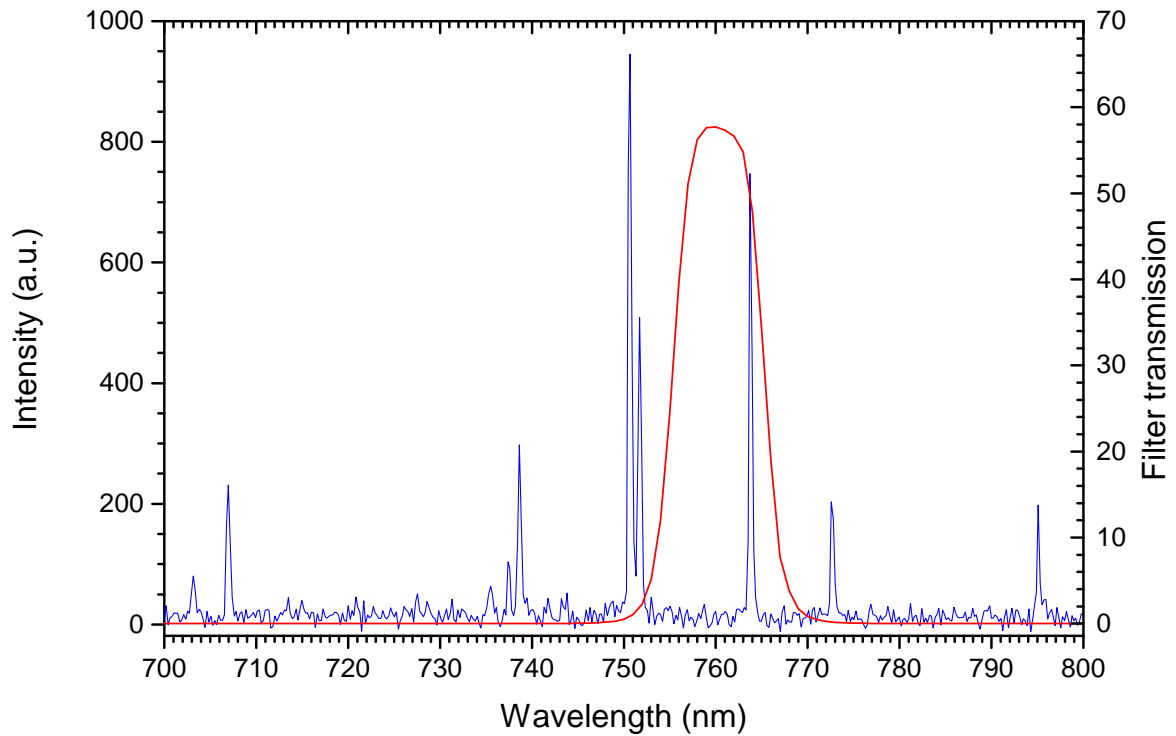

Figure 3.5 – In blue, the emission spectrum of the Ar/C_2H_2 plasma. In red, the transmission wavelengths of the argon line filter.The peak shown at 763.51 nm is used to measure the emission of the plasma. As shown, the peak at 763.51 nm is enclosed by the transmission of the filter.

Chapter 4

Results and discussion

4.1 Improving the microwave cavity

4.1.1 Mesh

All the equations and assumptions that have been explained in chapter 2 only apply to perfect circumstances.

Measurements showed that the cavity is not perfect: most peaks are not directly linkable to a theoretical mode. This is caused by imperfections in the cables, but also the imperfect symmetry of the cavity. A typical microwave spectrum is shown in figure 4.1 on the following page.
As shown in figure 4.1, the spectrum is full of different resonant modes. It is difficult to distinguish peaks. One of the reasons why the spectrum's peaks are hard to link to a theoretical mode is because the cavity is covered by a metal mesh. The side, but also the bottom of the cavity, is covered by this mesh. That is why one of the possible ways to improve the spectrum is to replace the metal mesh by solid aluminum.

4.1.2 Aluminum foil

To confirm whether the spectrum would improve by replacing the metal mesh by solid aluminum, aluminum foil was placed inside the cavity. Aluminum foil was placed on top of the bottom mesh and on the inside of the metal side mesh. The spectrum was measured three times as described in section 3.2. The result is shown in figure 4.2 on the next page.
As can be seen in figure 4.2, the cavity without the foil shows some extra peaks, especially in the higher frequency zone. The difference between the foil on top of the bottom plate and the foil on the side of the cavity is not clearly visible. Because the bottom aluminum foil improved the spectrum, the bottom metal mesh was replaced by a solid aluminum disc containing a regular grid of holes of 1 mm diameter. A photograph of the disc is shown in figure 4.3 on page 15. It seemed that placing the disc did have an effect on the spectrum. The resonant peaks in the higher frequency zone are still visible but are less in magnitude. The spectrum has also lost some peaks. See figure 4.4 on page 15 for a spectrum which the cavity contains the solid aluminum disc is measured.
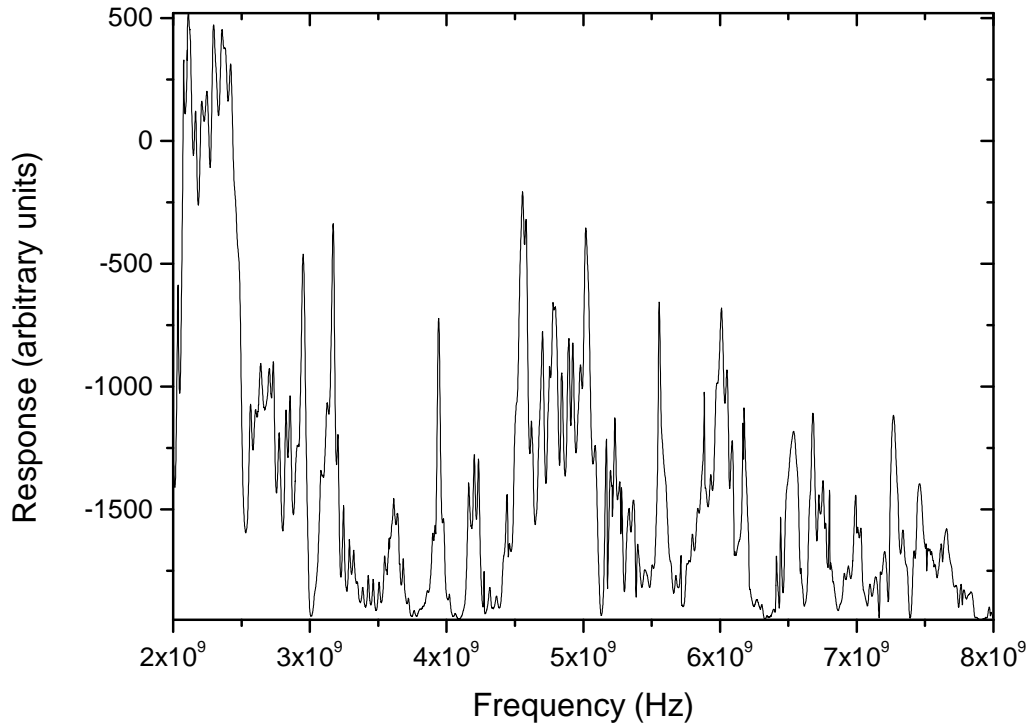
Figure 4.1 – The spectrum of the microwave cavity from 2-8 GHz.
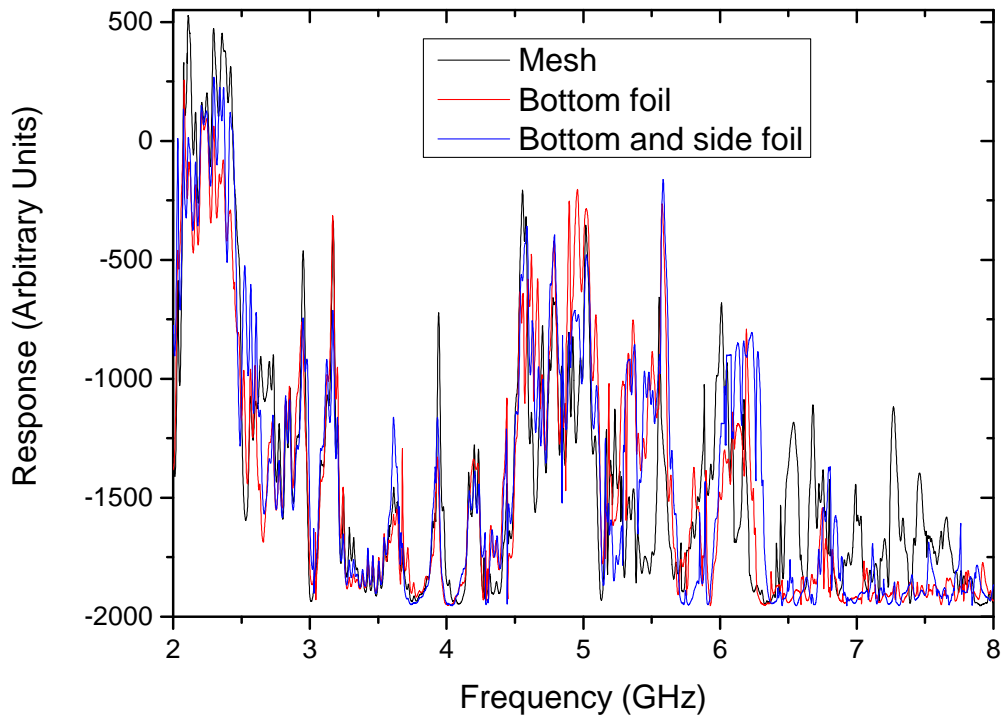
Figure 4.2 – The spectrum of the microwave cavity from 2-8 GHz. For some measurements foil was placed to confirm whether the spectrum would improve.

Figure 4.3 – A photograph of the solid aluminum disc. The antennas are also clearly visible.

Figure 4.4 – The spectrum of the microwave cavity from 2-8 GHz where the bottom mesh is replaced by a solid aluminum plate. The peaks in the higher frequencies are still visible but are lower in magnitude. The spectrum also lost some peaks.

4.2   MCRS using the PVC cube

4.2.1   Spectrum of the cavity from 6-6.5 GHz

As described in section 2.2.2, the theoretical frequency of a certain resonant mode can be calculated. Because the cavity is not ideal, it is not possible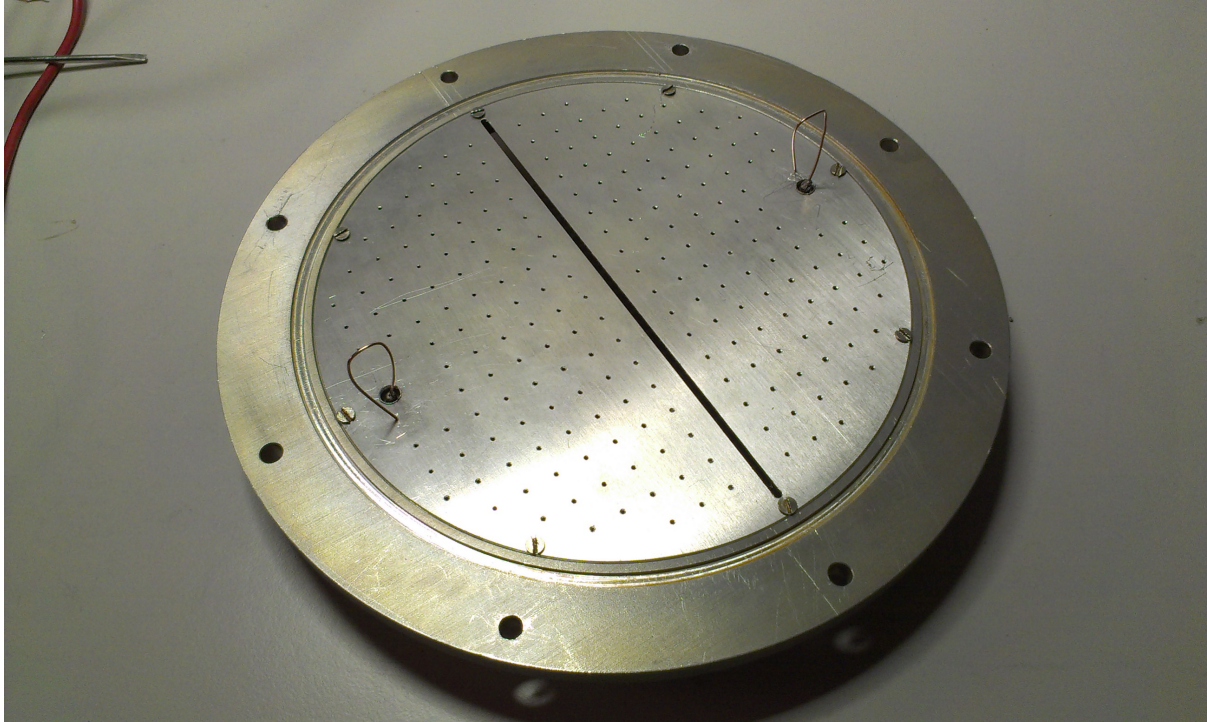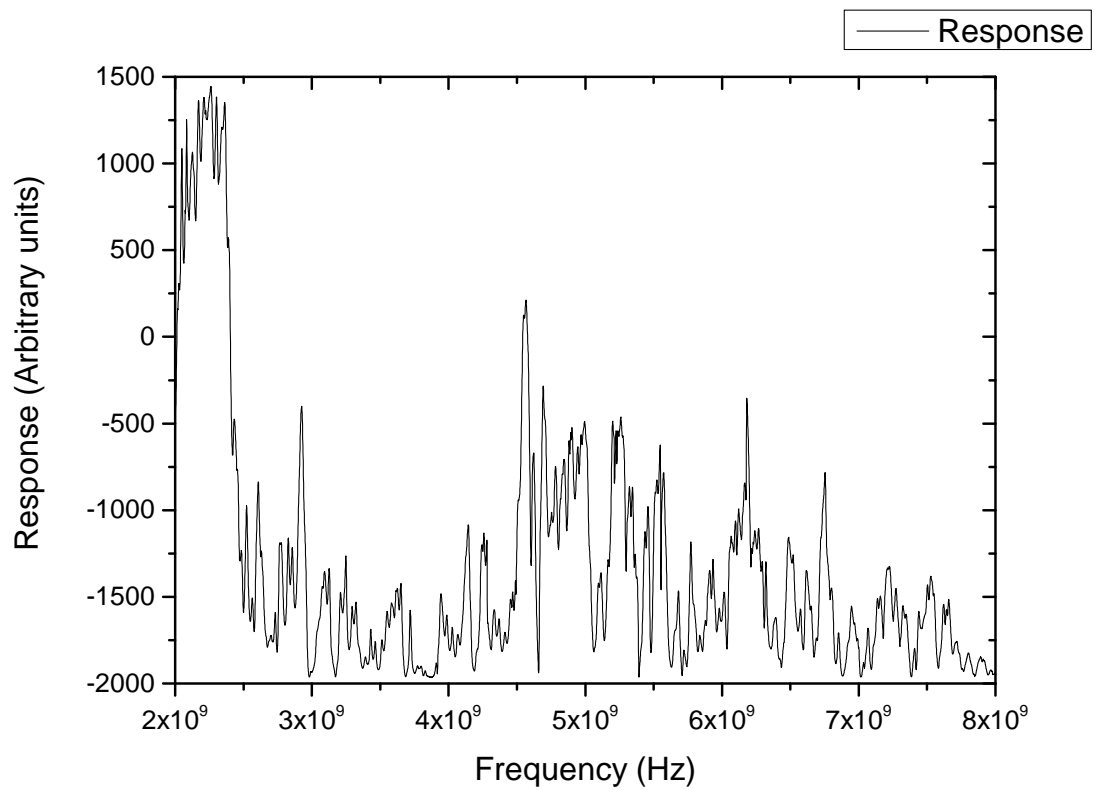 to directly link a certain resonance frequency to the correct TM_{mnp} or TE_{mnp} mode. As an example, figure 4.5 shows the spatial profile of the TM_{210} mode.

According to equation (2.22), the resonance frequency will shift as a function of the local electric field magnitude of the mode in question. When the PVC cube is moved across the cavity, it might be possible to link the right TM_{mnp} or TE_{mnp} mode to the right resonance frequency. The index p determines if the mode is height dependent, so the same measurement took place at different heights. The PVC cube's size is about 15 mm x 15 mm. The PVC cube is moved in the xy-plane at $x = 0$ (see figure 2.2 on page 4), while the antennas are located at $y = 0$.

A challenge that arises is that some peaks may overlap due to different resonance frequency shifts. Once peaks overlap, one can not distinguish them and the resonance frequency can not be measured. To determine which peak is a good one to analyze, the spectrum was again measured, but now in more detail and smaller frequency ranges. It seemed that the peak around 6.17 GHz was a proper distinguishable peak. The spectrum of 6-6.5 GHz is shown in figure 4.6 on the next page. It is measured in vacuum.
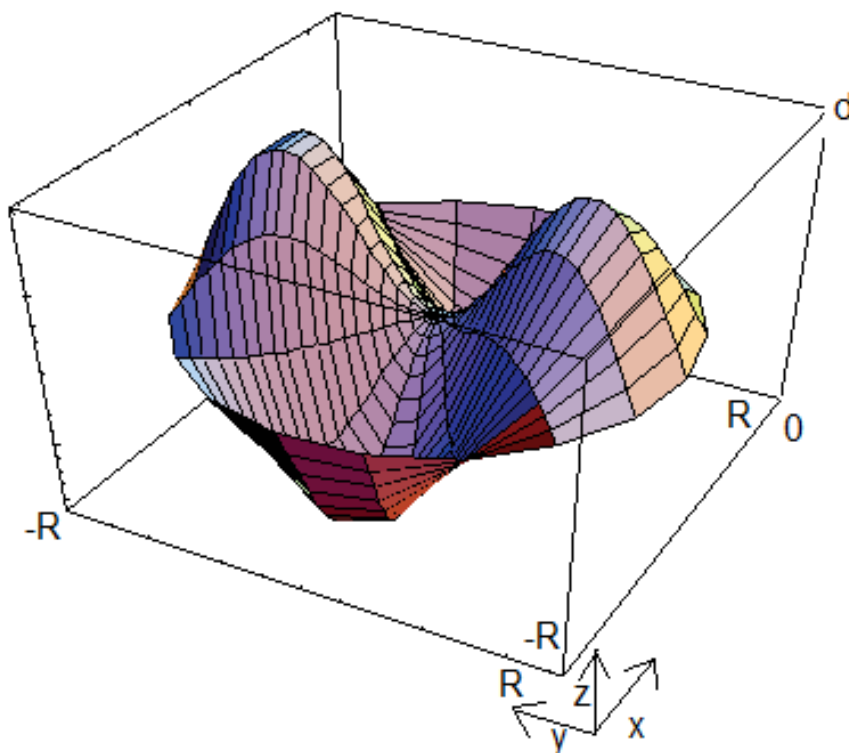

Figure 4.5 – TM_{210} mode spatial profile. Only E_z is present. The goal of these measurements is to create such an image out of the measurements. The TM_{210} mode is shown at one of its extremes. [7]
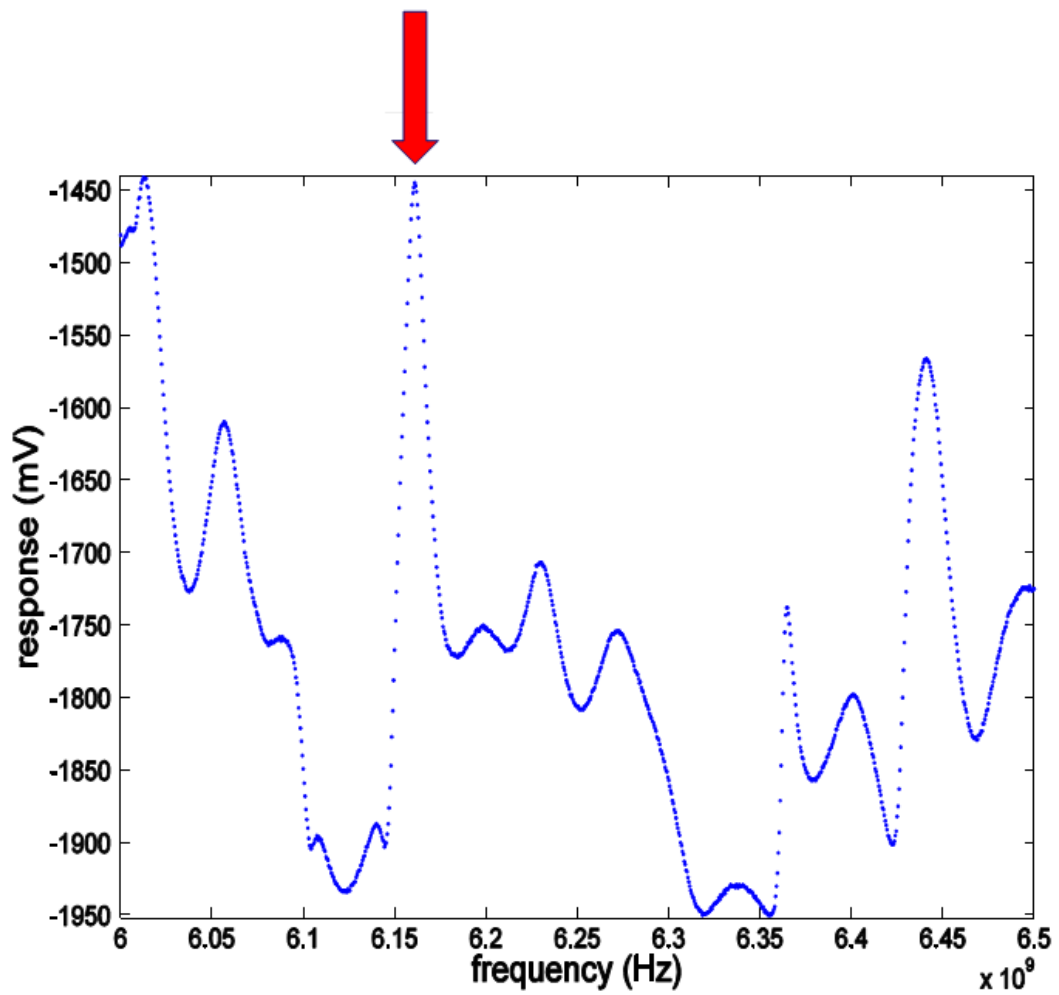
Figure 4.6 – The spectrum of the cavity. The highlighted peak around 6.17 GHz is clearly distinguishable from the rest.

4.2.2 Electric field of the resonance peak at 6.17 GHz

To match this mode to a theoretical mode, some theoretical resonant modes around 6.17 GHz are shown in figure 4.8 on the following page. The figure is retrieved by simulating equation (2.7) in Matlab. For exact details on the simulation, see appendix A. The finite size of the PVC cube is taken into account. They are simulated at $z = 0.75d$, which is at 75% height of the cavity, and through the xy-plane at $x = 0$.

The results of the measurements are shown in figure 4.7. As one can see, no mode directly matches the measured pattern shown in figure 4.7. Because the mode depends on the height (see figure 4.7), $p \neq 0$. This means TM_{420} falls out.

If TM_{412} is simulated at the same heights as the measurements are done, a qualitative agreement is found, see figures 4.9, 4.10 and 4.11. From these figures, the resonant mode at 6.17 GHz is believed to correspond to TM_{412}.
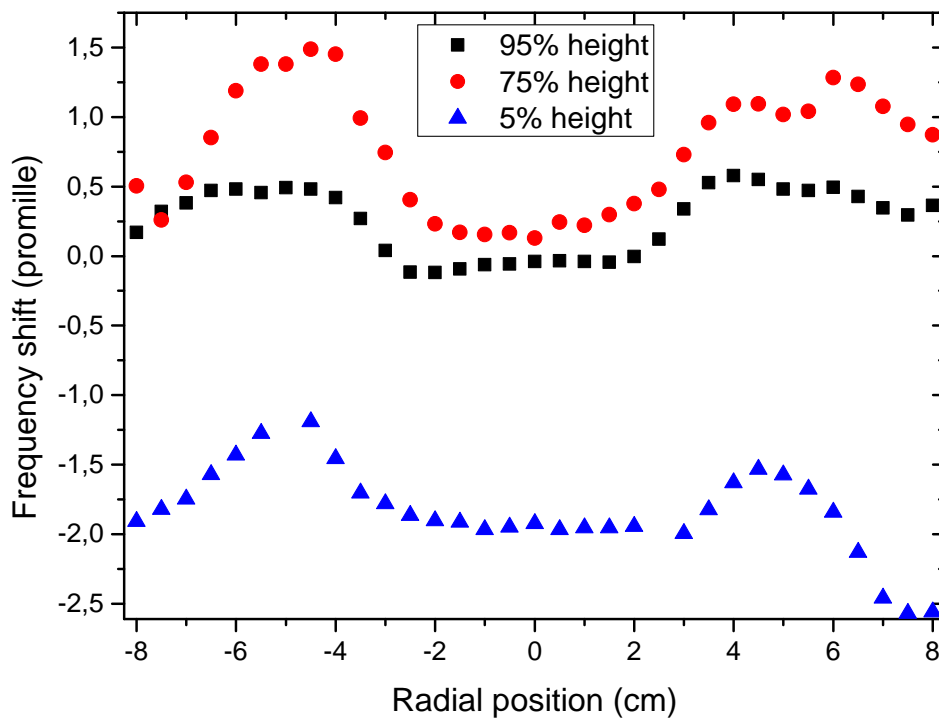
Figure 4.7 – The electric field of the cavity at the resonance frequency of 6.17 GHz. The modes look alike, but differ in magnitude.
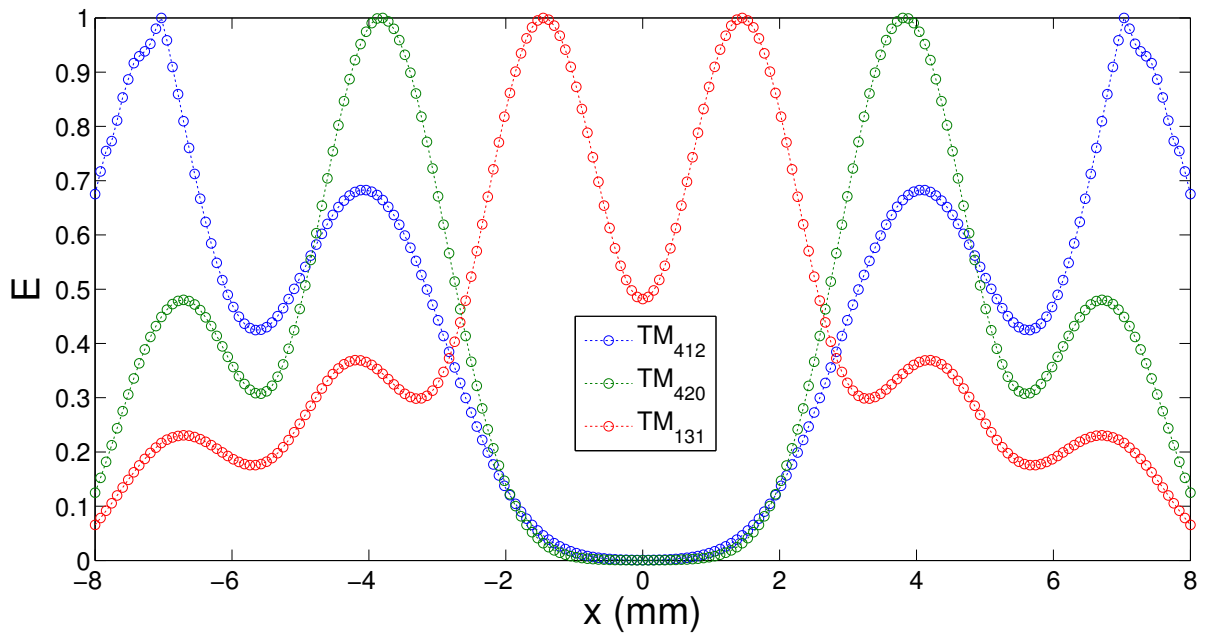
Figure 4.8 – Different theoretical TM modes around 6.17 GHz. They are simulated according to equation (2.7) and are simulated at the 75% height of the cavity and through the xy-plane at $x = 0$. For exact detail how this figure is constructed, see appendix A
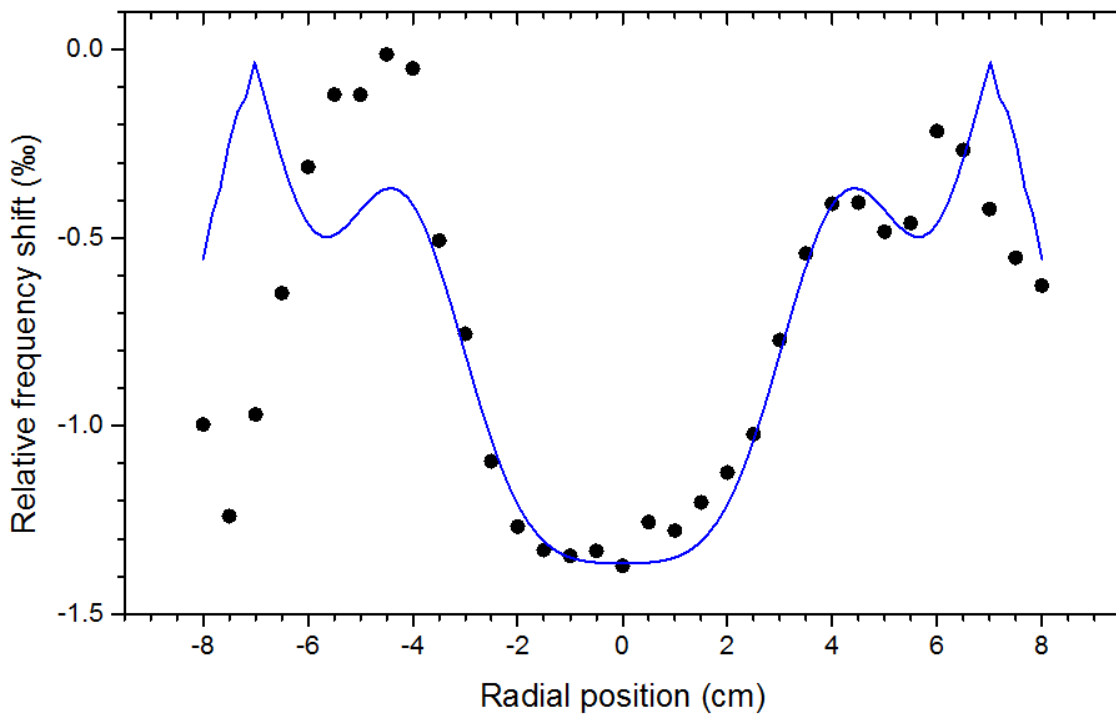
Figure 4.9 – The measured electric field at 75% height of the peak at 6.17 GHz and the simulated electric field at 75% height in one graph.
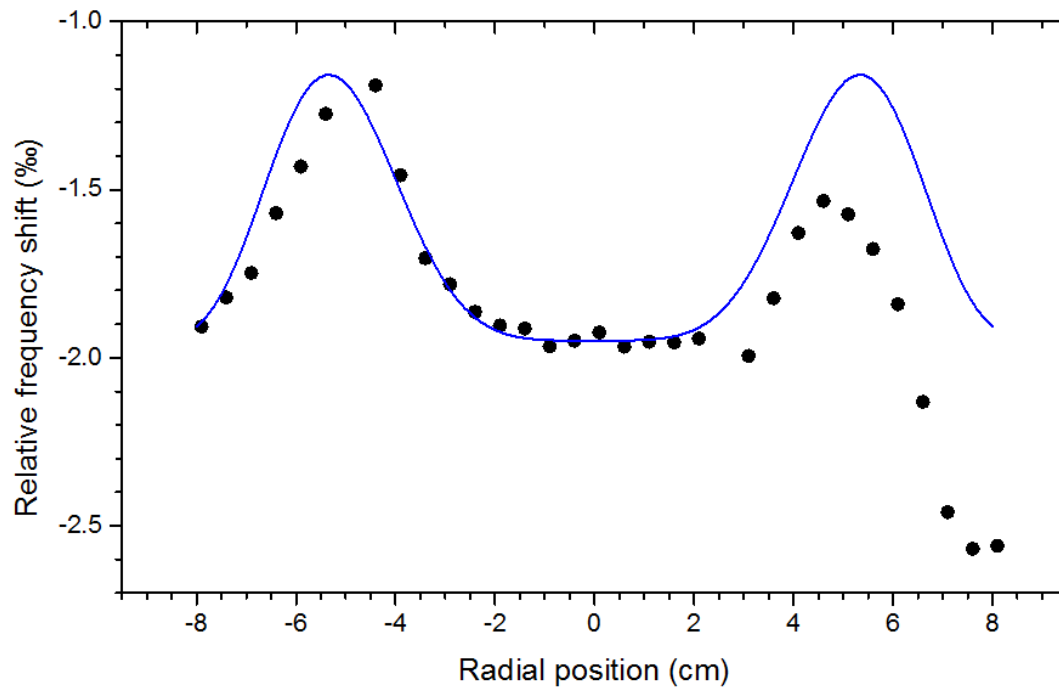
Figure 4.10 – The measured electric field at 5% height of the peak at 6.17 GHz and the simulated electric field at 5% height in one graph.
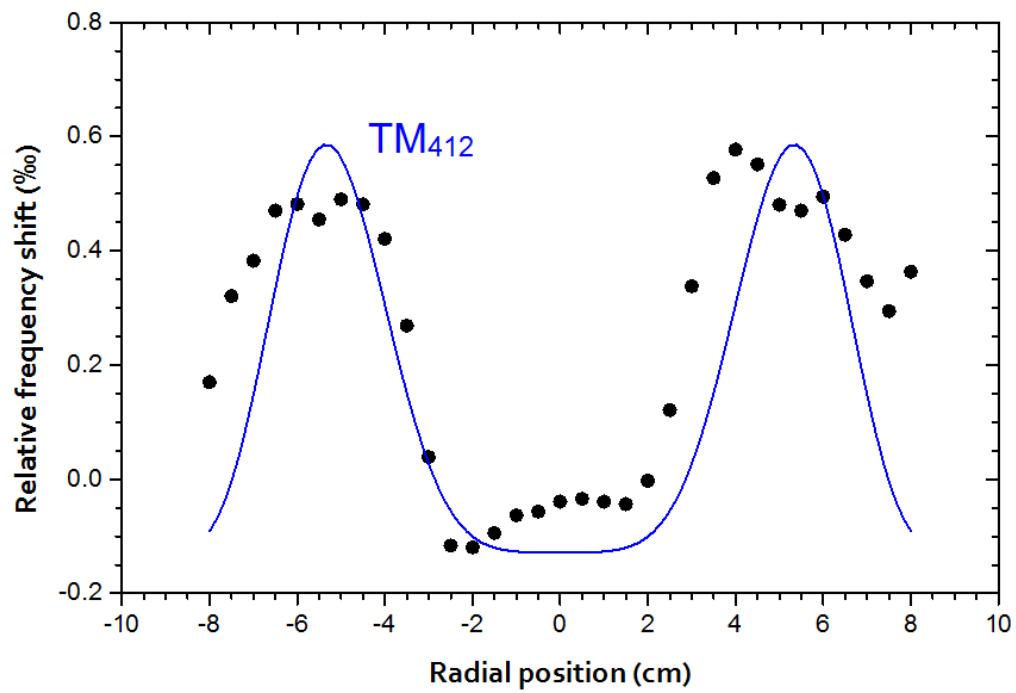
Figure 4.11 – The measured electric field at 95% height of the peak at 6.17 GHz and the simulated electric field at 95% height in one graph.

4.2.3 Electric field of the resonance peak at 6.2 GHz

The same measurements took place for a different peak, namely the peak next to the peak at 6.17 GHz. It is the small peak at 6.2 GHz, see figure 4.6 on page 17. The results at 75% have been removed due to overlapping peaks and thus indistinguishable resonance frequencies. The measurements again took place in the xy-plane at $x = 0$. The results are shown in figure 4.12.

Again, $p \neq 0$, because the profiles depend on the vertical position in the cavity. The simulated mode in section 4.2.2, see TM_{412} in figure 4.8 on page 19, showed a discontinuity at $\pm$ 7 cm. Because this discontinuity was also measured, see figure 4.9 on page 19, a coupling could be found. The peak measured in this section doesn't show any discontinuities. Therefore, and because the measurements only took place in the xy-plane at $x = 0$, a one-to-one coupling between the simulated modes and the measured electric field could not be found. For more explanation, see section 4.2.4.
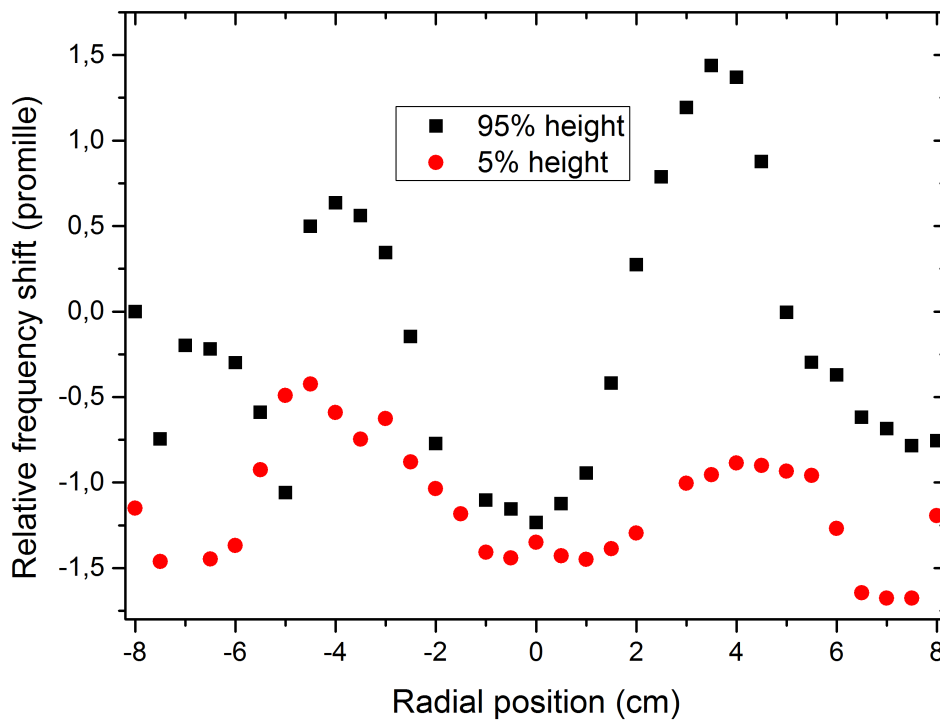
Figure 4.12 – The electric field of the cavity at a resonance frequency of 6.2 GHz. The same as in figure 4.7, the modes look alike but differ in magnitude

4.2.4 Discussion

The previous paragraph stated that a one-to-one coupling of measured to theoretical modes was hindered by the unavailability of a measurement in the x-plane. Figure 4.13 visualizes why a measurement in the x-plane would be beneficial.. It shows a 2D electric field profile of the TM_{131} mode. This mode has its theoretical resonance frequency at 5.94 GHz. It is simulated in MATLAB. For exact details on the simulation, see appendix A.

If a cross-sectional graph is taken through the xy-plane and at $x = 0$, it is clear that the same graph is produced as in figure 4.8 on page 19. However, figure 4.13 also shows that there is actually no electric field when a cross-sectional graph is taken through the xy-plane at $y = 0$. If the measurements that are shown in figure 4.12 on the previous page would have been repeated in the perpendicular plane, more information could have been retrieved about which mode is linked to the measurements. If there was an electric field, TM_{131} can be excluded. If there was no electric field, the possibility of the mode being TM_{131} would be much larger.
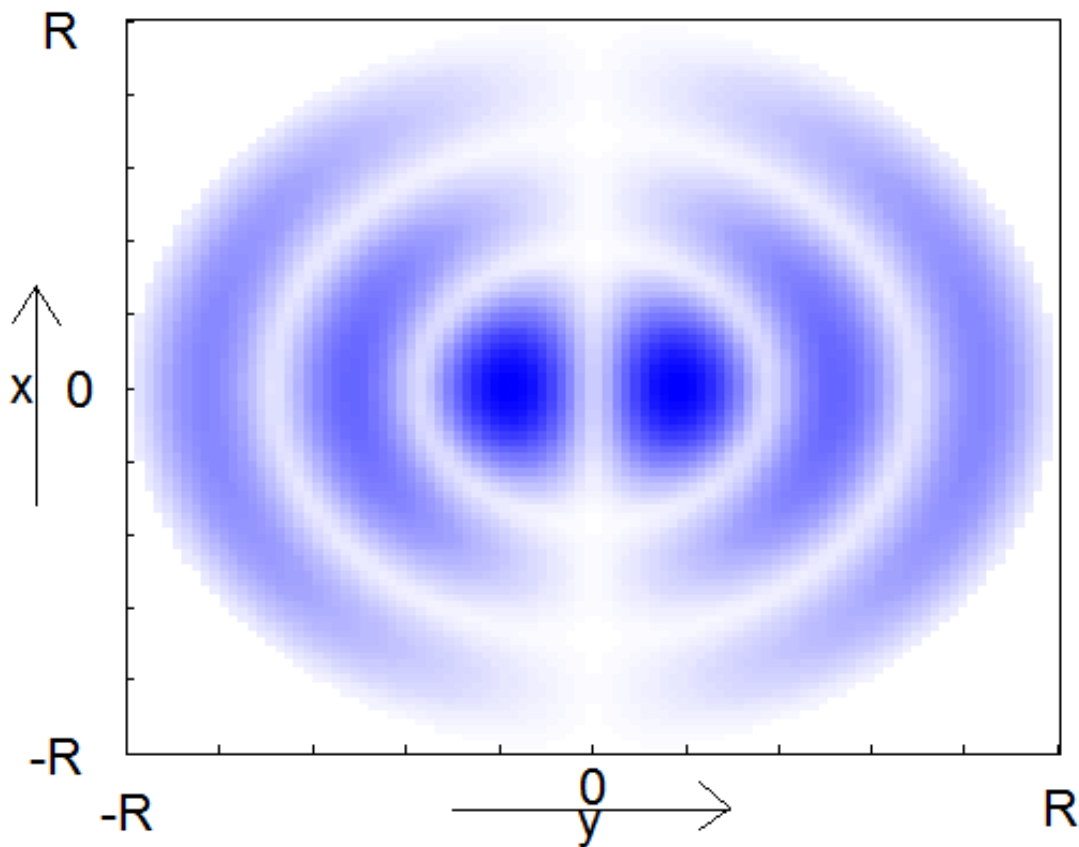
Figure 4.13 – The 2D electric field profile of the TM_{131} mode at 80% height of the cavity. For exact details on how this figure is constructed, see appendix A.

4.3 Scattering and electron density

As explained in section 3.3.2, the scattering by the dust particles can be measured using one of the cameras. When time continues, the void should become visible by a dark spot inside the cavity, because there are no dust particles in the void.

One frame recorded by the camera of the scattering is shown in figure 4.14.
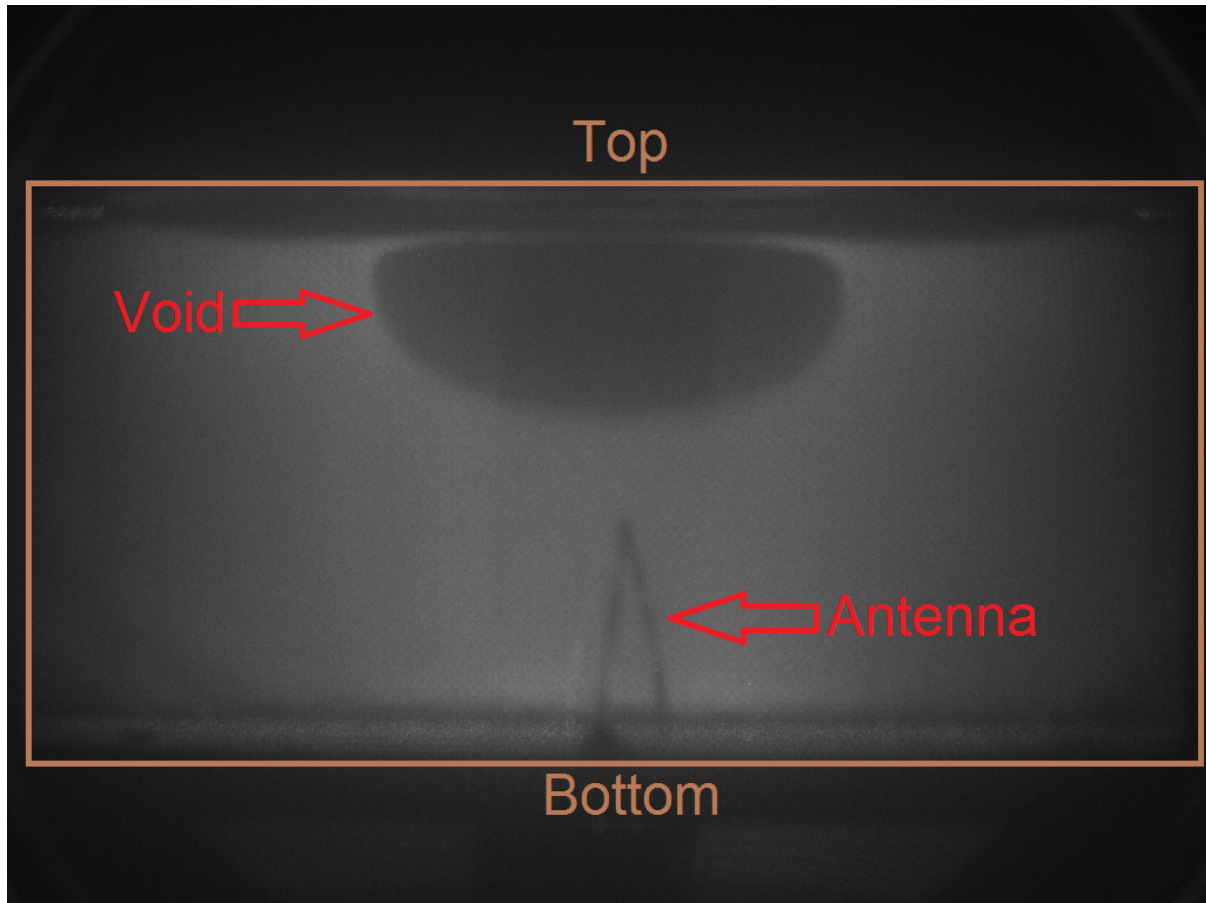
Figure 4.14 – A scattering frame recorded by the camera. In brown, the cavity's geometry is shown. In the bottom an antenna is clearly visible. The dark ellipsoid-shaped zone is the dust-free void. The frame is background corrected.

The experiment of the scattering is accompanied by the electron density measurements described in section 3.2. The void size can be tracked in time using Canny edge detection. For exact details on the Canny edge detection, see appendix C. The electron density was determined at a resonance peak of 7.505 GHz. To analyze the frames recorded by the CMOS the frames are background corrected. This is done by averaging the pixels of the frames up to plasma ignition and substracting the result from the other frames. A Savitzky-Golay filter has been used to retrieve the electron density (red graph). The light blue graph shows the raw data. The result is shown in figure 4.16 on the following page.

As can be clearly seen in figure 4.16, the void size increases in time. Suddenly it shrinks and start growing again. The process is reproducible. A zoom-in of figure 4.16 at a point where the hiccup occurs is shown in figure 4.15. Again a Savitzky-Golay filter is used to retrieve the red electron density graph. The different regions in figure 4.16 and 4.15 are explained below.

Region **I**: In the first couple of seconds after plasma ignition, negative ions will form (see equation (2.2). This will ultimately result in a decrease of free electron density. As was discussed in section 2.1, at a certain point the particles will transit into the coagulation phase. This phase is associated with the so-called $\alpha - \gamma'$ transition [10] and is characterized by a sudden decrease in electron density and increase in electron temperature. At a more elementary level this means that the electron losses on the particle exceed the electron losses on the discharge chamber's walls. From figure 4.16 it can be estimated that coagulation sets in after about 10 s after the ignition of the plasma. In other words, this is the time it takes for the proto-particles to reach the critical density needed for coagulation to occur.

Region **II**: When dust particles suddenly leave the discharge chamber because they become too large, the electron sink decreases in strength. The expanding void itself can also be the reason for particles being expelled from the discharge. Since particles feel each due to their negative charge, particles being pushed downwards at the void boundary can push lower particles out of the discharge in a manner comparative to falling dominoes. Since it takes time for the plasma to respond to this new situation, the electron density will briefly go up, until ionization is at an equilibrium value again. That is why a temporal increase in the electron density is seen. To explain the expansion of the void, the forces inside a plasma need to be described. For exact details on which forces act inside the plasma, see Job Beckers [11]. Once the dust particles reach a critical size, r_{crit} (see section 2.1), the ion force exceeds the electric force. The ion force is a force which is directed outward of the void while the electric force is directed from the cavity's walls towards the center of the cavity. Because the ion force exceeds the electric force, the void will expand.

Region **III**: Region II shows an increase in the void size. Region III shows a decrease. Together they form the hiccup. The ion force, see region **II**, is a force which is directed outward of the void. Once the dust particles enter the coagulation phase, the ion force will drop. Due to this drop in the ion force, the void will shrink.
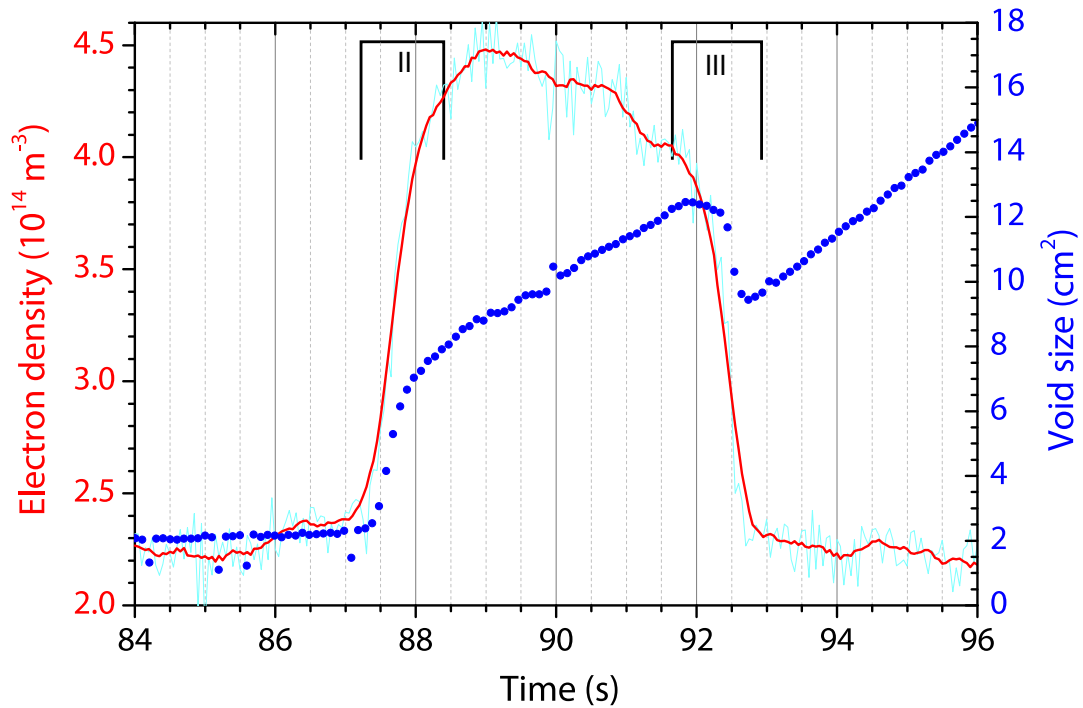
Figure 4.15 – A zoom in of figure 4.16. A Savitzky-Golay filter has been used to retrieve the electron density (red graph). The light blue graph shows the raw data. The hiccup and the electron density are correlated. Once the void sizes increases, so does the electron density. Once the void size decreases, so does the electron density. The region where the hiccup occurs has been split into two parts. They are now to referred to as region **II** and **III**.
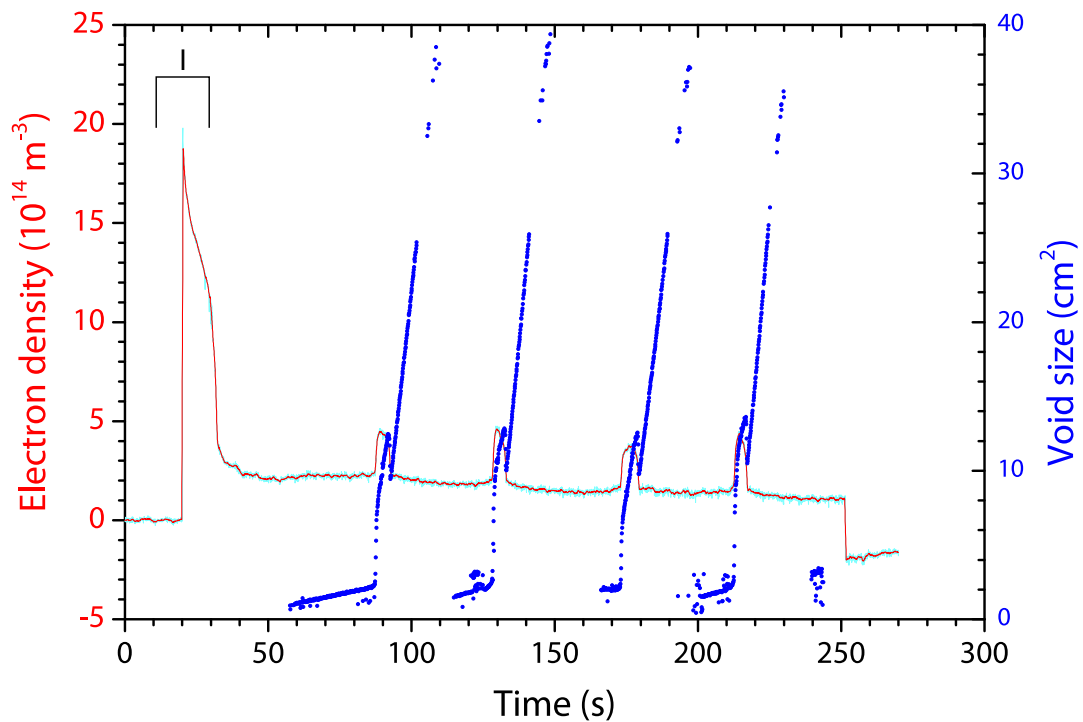
Figure 4.16 – The void size, tracked in time using Canny edge detection, and the electron density (for a resonance peak at 7.505 GHz) in one graph. A Savitzky-Golay filter has been used to retrieve the electron density (red graph). The light blue graph shows the raw data. The region where the electron density heavily increases and decreases is now to referred to as region **I**.

4.4 Emission and electron density

Section 3.3.1 describes how the emission measurements are done. The emission measurements are accompanied by the electron density measurements described in section 3.2. To analyze the frames recorded by the CMOS the frames are background corrected. This is done similar to the scattering experiments described in section 4.3

One frame which is recorded by the camera is shown in figure 4.17.
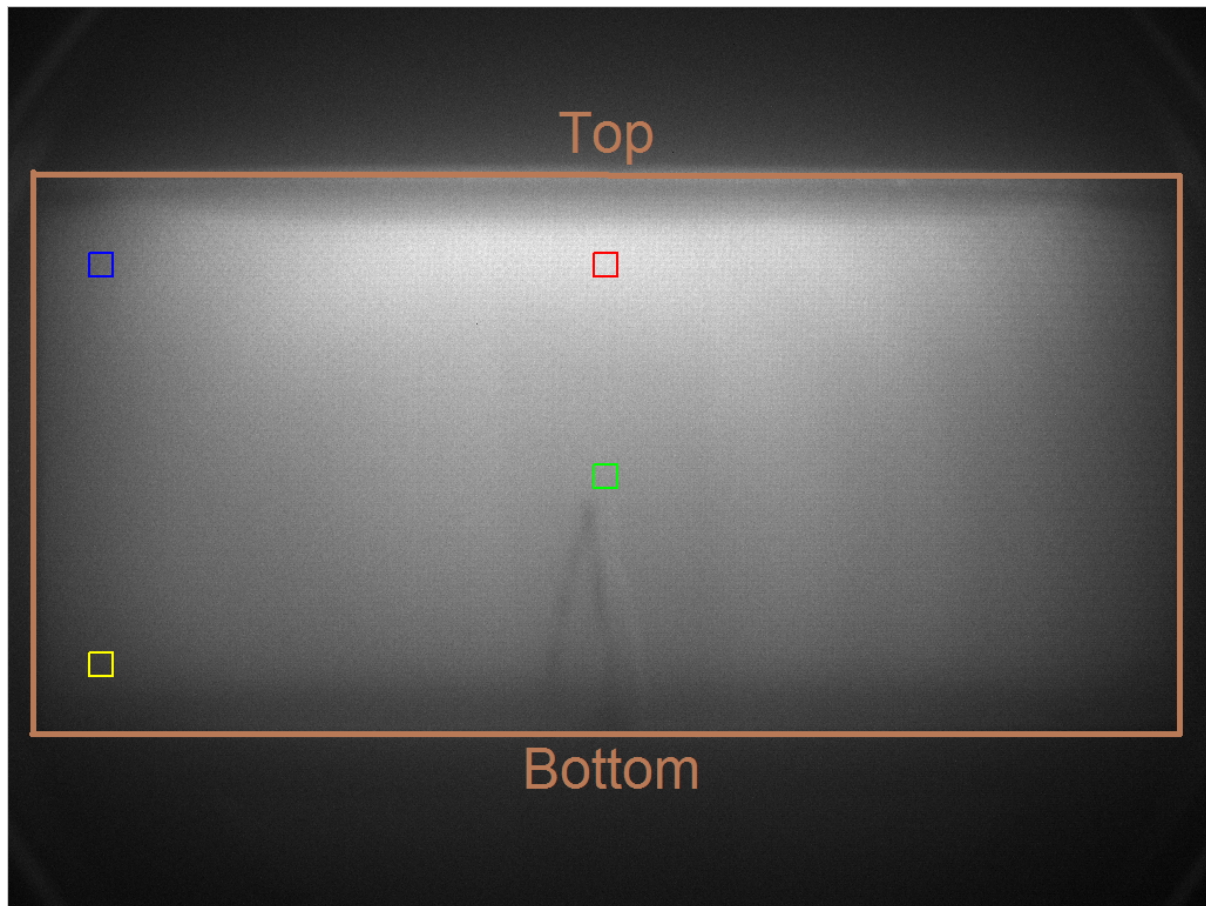
Figure 4.17 – An emission frame recorded by the camera. The ROIs (Regions of Interest) are highlighted to show where the emission is averaged. In brown the cavity's geometry is displayed. The frame is background corrected.
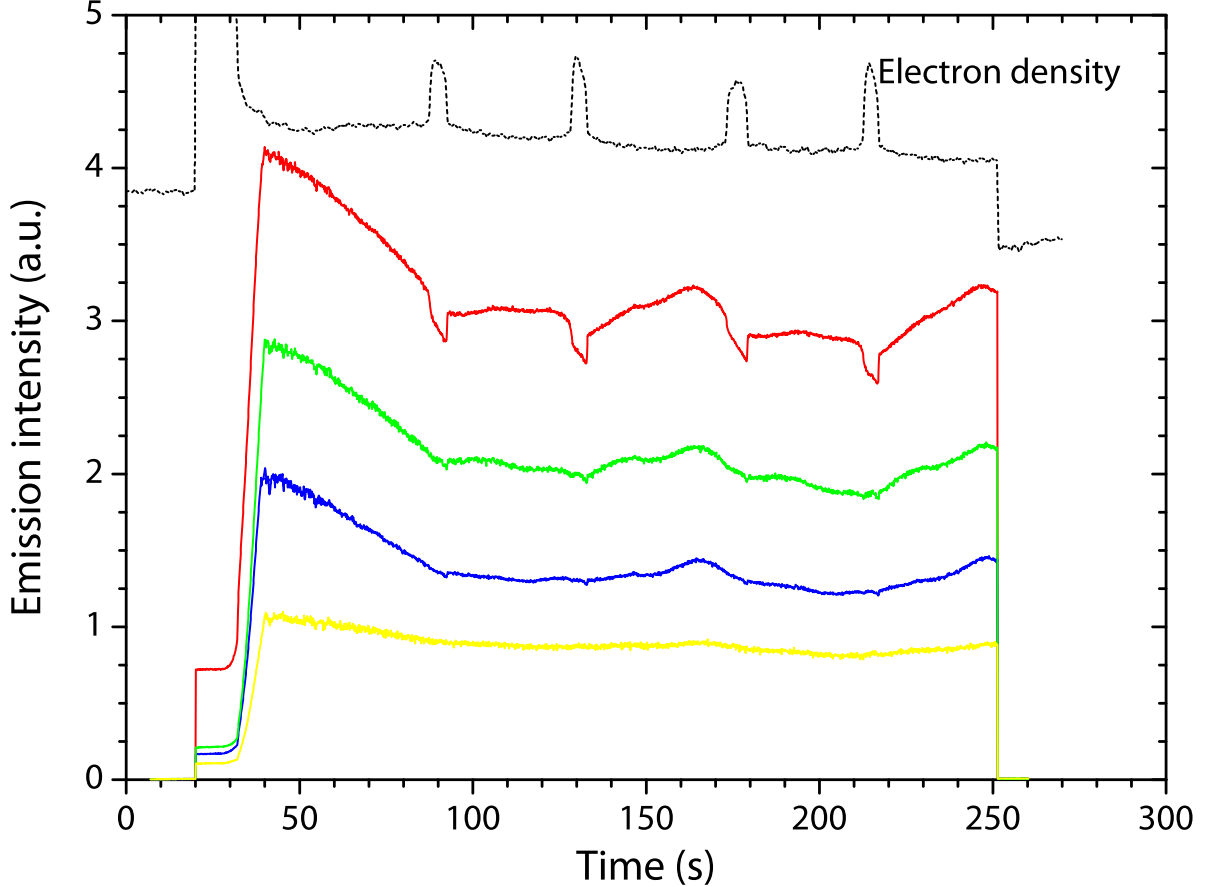
Figure 4.18 – In black, the electron density at a resonance peak of 7.505 GHz. The colored graphs are the averaged emission across the different ROIs, see figure 4.17. The electron density is rescaled for clarity.

Because of noise the emission value is averaged across several pixels (20x20) inside an image recorded by the camera. In figure 4.17, the highlighted squares show from which pixels the emission is averaged. As can be seen in figure 4.14 on page 23, some squares lie inside the void and some squares lie outside the void. The result for the different ROIs (regions of interest) as well as the electron density is shown in figure 4.18.

A zoom in of figure 4.18 is shown in figure 4.19.

The different regions in figure 4.17 and 4.19 are explained below.

Region **II**: The same effect happens to the electron density as described in section 4.3. Dust particles leaving the discharge chamber will temporarily lead to an increase of the electron density. A steady decrease of the emission is observed up to the start of phase **III**.

Region **III**: The hypothesis for this region is a new coagulation phase occurring inside the void. The C_2H_2 flow is constant, so the fresh supplied molecules can start a new growth phase. However, in the dusty region they are efficiently adsorbed on the dust partices. As a result, in a dusty region no new cycle can start and one generally ends up with a fairly monodisperse size distribution of dust particles. In contrast, in the void region there are no dust particles so a new cycle can - and will - start. Once this new cycle reaches the coagulation phase, the electron density will go down, as earlier discussed (see section 2.1). Due to this decrease in electron density, the plasma will respond by increasing the electron temperature. This is what is called the $\alpha - \gamma'$ transition [10]. As a result of an increased electron temperature, the plasma will emit more photons if the argon line in question is particularly sensitive to electron temperature changes. Because a clear increase in emission is seen in figure 4.19, the argon emission line at 763.51 nm is sensitive to electron temperature.

As one can see in figure 4.18, no clear increases in emission are measured in the other ROIs than the red square. This shows that the increase in emission is particularly situated inside the void. In other words, the coagulation phase of a new batch of C_2H_2 happens inside the void. Figure 4.18 clearly shows that the emission is space dependent. The closer to the void, the more the emission will increase.

To confirm this, the emission of the whole plasma before the start of the hiccup ($\pm$ 91.8 s) is substracted from the emission after the end of the hiccup ($\pm$ 92.9s). Now the whole plasma is taken into account and no different ROIs are taken as done before. The result is shown in figure 4.20 on the following page. This confirms that the increase of emission is indeed located mostly within the void. This supports the hypothesis that coagulation happens inside the void when the hiccup occurs. As shown in figure 4.20, the plasma's increase of emission inside the void is higher than the plasma's decrease of emission outside the void.
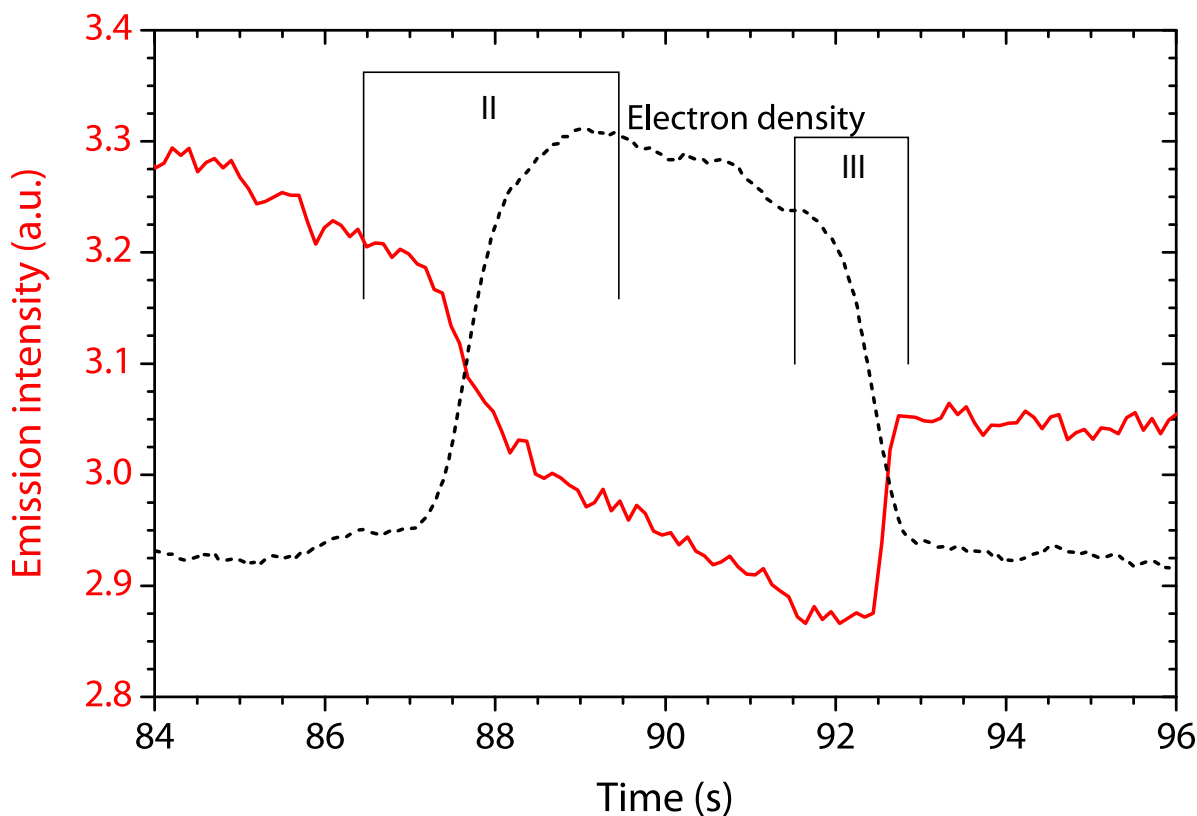
Figure 4.19 – A zoom in of figure 4.18 around the first hiccup of the emission. Emission from the red ROI is shown together with the (rescaled) electron density. The electron density is retrieved out of the raw data using a Savitzky-Golay filter. For reference with section 4.3, the region where the electron density increases is denoted by region II and the region where the electron density decreases is denoted by region III.
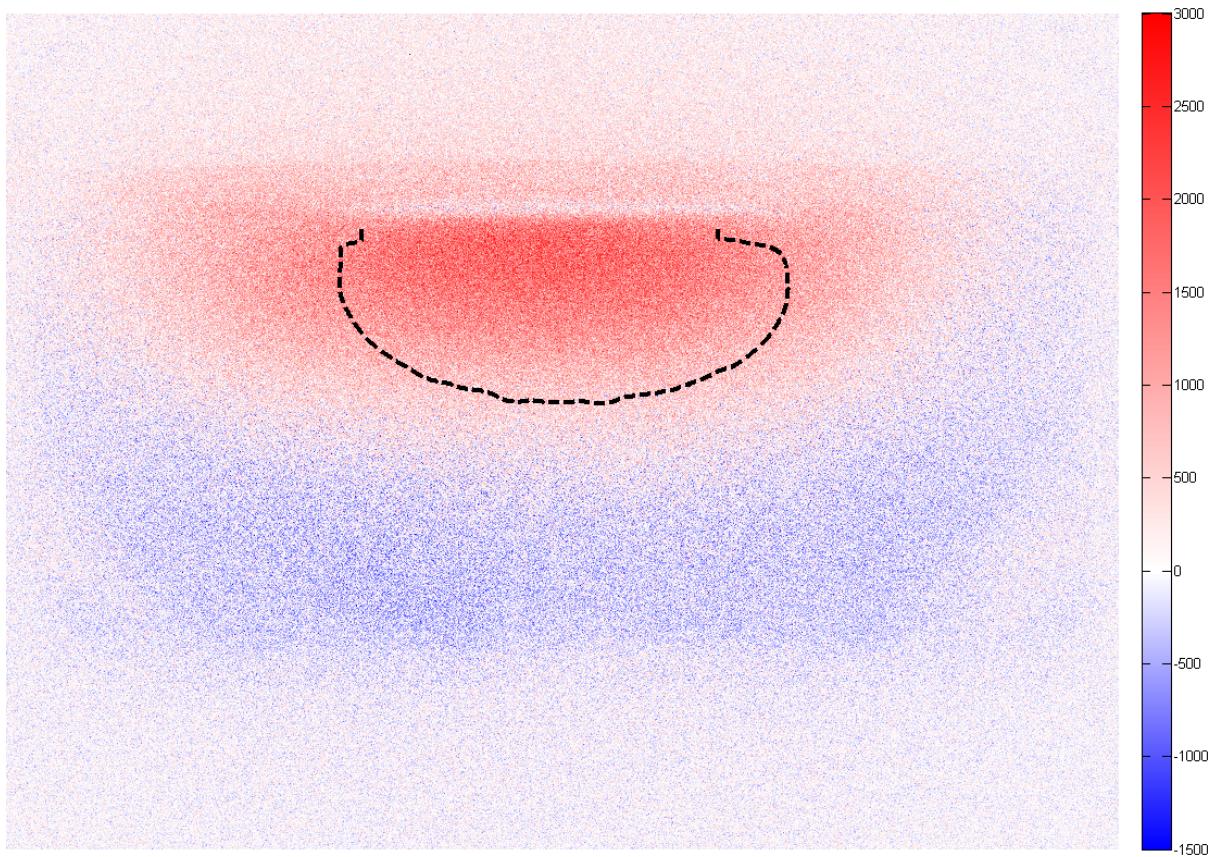
Figure 4.20 – The difference in emission of the whole plasma at the beginning of the hiccup substracted from the emission at the end of the hiccup, see figure 4.19. Red means an increase en emission and blue is a decrease in the emission. The black dots mark the region of the void. One can clearly see an increase of emission inside the void. In some regions the emission even drops. Note that the increase of emission inside the void is larger than the decrease in emission outside the void.

Chapter 5

Conclusions and recommendations

In this research there are several things to conclude. First of all the microwave cavity resonance spectrum shows a lot of different modes because the cavity is rather big and surrounded by a mesh. Due to this the cavity is difficult to study. A smaller cavity which is surrounded by solid metal would probably show less modes. Because of this it was a challenge to connect a measured mode to the corresponding theoretical mode.

The Microwave Cavity Resonance Spectroscopy using a PVC cube is a good way to determine the electric field profile of a certain resonant mode. By locally disturbing the electric field using a dielectric, the electric field profile can be determined. The resonant mode of the cavity at 6.17 GHz is believed to correspond to TM_{412}. One problem that arised when we tried to connect the other measured peak to the corresponding theoretical mode was the lack of measurement directions. We only moved the PVC cube in one plane and by doing this we only retrieved two dimensional information about the electric field profile of the resonant mode. A future recommendation is therefore to, whenever an experiment involves this technique, measure in different directions so a three dimensional electric field profile can more easily be constructed.

The emission and scattering measurements combined with the electron density measurements of the plasma gave a lot of information about what was happening inside the plasma and the void. By studying the four phases of dust particles growth, the various remarkable regions in the graph could be described. After a quick rise in electron density the electron density suddenly drops till it reaches an equilibrium. The drop is associated with the so-called $\alpha - \gamma'$ transition [10] and the fact that the growing dust particles start to act as an electron sink. When these particles suddenly leave the discharge chamber the sink is gone and the plasma will react by temporarily increasing the electron density of the plasma. This is shown by small bumps in the electron density graph.

When locally determining the emission of the plasma, one can see a peculiar effect. The emission of the plasma inside the void shows clear increases while the emission outside the void does not. The hypothesis for this effect is a new coagulation phase occuring inside the void. The inserted precursor molecules and/or radicals are efficiently adsorbed on the dust particles in the dusty region. In the void there are no dust particles so the inserted precursor molecules and/or radicals can and will start a new growth phase inside the void. Once this new growth cycle reaches the coagulation phase, the electron density will go down. Due to this decrease, the electron temperature will go up. The plasma will emit more photons if the argon line in question (in our case 763.51 nm) is particularly sensitive to electron temperature changes. Because an increase in emission is measured, it is clear that the argon emission line at 763.51 nm is sensitive to fluctuations in the electron temperature.

Bibliography

[1] F.M.J.H. van de Wetering. Ethynyl anion dynamics in the first 10 milliseconds of an argon-acetylene radio-frequency plasma. Master's thesis, Eindhoven University of Technology, 2011.

[2] J. Perrin and C. Hollenstein. *Dusty Plasmas: Physics, Chemistry and Technological Impacts in Plasma Processing*. Wiley, 1999.

[3] K. De Bleecker, A. Bogaerts, and W. Goedheer. Detailed modeling of hydrocarbon nanoparticle nucleation in acetylene discharges. *Physical Review E*, 73:026405, 2006.

[4] D.J. Griffiths. *Introduction to Electrodynamics*. Addison Wesley, 4th edition, 2013.

[5] I.G. Wilson, C.W. Schramm, and J.P. Kinzer. High Q resonant cavities for microwave testing. *Bell System Technical Journal*, 25(3):408–434, 1946.

[6] R.A. Adams and C. Essex. *Calculus, A complete course*. Pearson Education Canada, 7th edition, 2009.

[7] M. Sorokin. *Dust particle formation in silane plasmas*. PhD thesis, Eindhoven University of Technology, 2005.

[8] C.F. Bohren and D.R. Huffman. *Absorption and Scattering of Light by Small Particles*. Wiley-VCH, 1983.

[9] J.B. Boffard, R.O. Jung, C.C. Lin, and A.E. Wendt. Optical emission measurements of electron energy distributions in low-pressure argon inductively coupled plasmas. *Plasma Sources Science and Technology*, 19(6):065001, 2010.

[10] A.A. Fridman, L. Boufendi, T. Hbid, B.V. Potapkin, and A. Bouchoule. Dusty plasma formation: Physics and critical phenomena. Theoretical approach. *Journal of Applied Physics*, 79(3):1303–1314, 1996.

[11] J. Beckers. *Dust Particle(s) (as) Diagnostics in Plasmas*. PhD thesis, Eindhoven University of Technology, 2011.

Appendix A

Simulating the two dimensional electric field profile using Matlab

To simulate figure 4.13 on page 22, the following script is used. The entries of the function plotEPlane are modeString, planeDef, pos, steps. The script calculates the electric field E. modeString defines the specific mode, thus TM_{mnp} or TE_{mnp}. planeDef defines the plane which remains constant. pos is the relative position inside the cavity. This means $-1 < x < 1$, $-1 < y < 1$ and $0 < z < 1$. Steps means the number of discretations. The script makes use of a function named cavResFunction, which calculates the electric field from equation (2.7).
To illustrate this, figure 4.13 was constructed by using

E=plotEPlane('TM131','z',0.8,100);

The matrix E (100x100) is now filled and can be plotted. By doing this, the theoretical two dimensional electric field profile at 80% height of TM_{131} is constructed. Note that in this script, the finite size of the PVC cube is not taken into account.
The exact script which is used for calculating the electric field is shown below.

```
function [E_mag, h] = plotEPlane(modeString,planeDef,pos,steps,varargin)
%PLOTEPLANE   Plot a translucent plane of given orientation in 3-D space of
%which the transparency is a measure of the magnitude of the electric field
%for the given resonant mode (transparent: E is zero, opaque: E = E_0).
%
%   [E_mag, h] = PLOTEPLANE(modeString,planeDef,pos,steps) adds a blue plane
%     with 0.5 pt black edges to the CURRENT figure. If no figure exists,
%     Matlab creates one.
%     Inputs:
%     modeString: string signifying the resonant mode in the form 'TMmnp'
%     or 'TEmnp', with m,n,p integers, e.g. 'TM123'.
%     planeDef: string indicating the plane in 3-D space to plot. Possible
%     values are 'x' (for an yz-plane at constant x), 'y' (for an xz-plane
%     at constant y), 'z' (for an xy-plane at constant z), and 'angle' (for
%     a vertical plane crossing the axis of the cavity and making a
%     constant angle with the xz-plane.
%     pos: the position to plot the plane at. For planeDef = 'x', 'y', or
%     'z' this means the (normalized) position the plane is plotted at
%     along this dimension. For example, planeDef = 'y' and pos = 0.5 means
%     an xz-plane at y = 0.5. If planeDef = 'angle', pos is the angle in
%     degrees measured from the xz-plane towards positive y.
%     steps: integer denoting the number of discretization steps on which
%     the electric field is calculated. It is a measure for the resolution
%     of the resulting field plot (containing steps^2 pixels in
%     total). Good starting values are between 100 and 200.
%     Outputs:
%     h: the object handle to the drawn surface. Running delete(h) will
%     remove the drawn plane from the current figure.
%     E_mag: the calculated 2-D array (image) of the electric field
%     distribution.
%
```

```matlab
%     PLOTEPLANE(...,surfColor) will give the plane the color given by
%     the 3-element RGB vector surfColor, e.g. surfColor = [1 0 0] will
%     color the plane red. Note that you CANNOT use Matlab's (shortened)
%     string versions of the colors (e.g. 'r' or 'red' for the example
%     above).
%
%     PLOTEPLANE(...,surfColor,borderColor) as above, but this will color
%     the plane edges with the given color. borderColor accepts all
%     Matlab's colorspec values: RGB triplets or (shortened) strings, e.g.
%     [0 1 0], 'r' or 'red' for a red border. If you do not want a border
%     around the plane use borderColor = 'none'.
%
%     PLOTEPLANE(...,surfColor,borderColor,borderWidth) as above, but this
%     will make the plane border of width borderWidth in points.
%
%   Example:
%   PLOTEPLANE('TM123','angle',20,200,[0 1 0],'r',.25) plots a vertical
%   plane at an angle of 20 degrees with a resolution of 200*200 pixels.
%   The plane will have a green color and a red border of width 0.25 pt.

% Author: FMJH van de Wetering
% Date: 17-Sept-2013 16:29 LT
% Revision: 0.15

% Check for a valid planeDef
if ~strcmp(planeDef,'x') && ~strcmp(planeDef,'y') && ~strcmp(planeDef,'z')...
        && ~strcmp(planeDef,'angle')
    error('Invalid plane definition. Valid values are ''x'', ''y'',''z'' or ''angle''')
end

% variable input arguments
switch length(varargin)
    case 0
        surfColor = [0 0 1];
        borderColor = 'k';
        edgeWidth = .5;
    case 1
        surfColor = varargin{1};
        borderColor = 'k';
        edgeWidth = .5;
    case 2
        surfColor = varargin{1};
        borderColor = varargin{2};
        edgeWidth = .5;
    case 3
        surfColor = varargin{1};
        borderColor = varargin{2};
        edgeWidth = varargin{3};
end

E_max = 1;

% What plane to calculate en plot depends on the given planeDef variable
switch planeDef
    case 'z' % An xy-plane at constant height (z)
        E_mag = zeros(steps,steps); % Pre-allocate the magnitude of the electric field, E_mag.
                %It's a square 2-D array (image), with step*step elements.

        % (Double) loop over the x and y direction and populate E_mag
        k = 1; % k is the first index of E_mag(k,l) associated with the x-direction
        waitH = waitbar(0,'Running...');  % Construct a progress bar
        for x = linspace(-1,1,steps) % We want to calculate the distribution of E_mag over
                %-1 < x < 1, where the radius of the cavity is set to 1.
            mess = sprintf('Running... (%d/%d)',k,steps);  % Update the progress bar
            waitbar((k-1)/steps,waitH,mess) % Ditto
            l = 1;  % l is the second index of E_mag(k,l) associated with the y-direction
            for y = linspace(-1,1,steps) % We want to calculate the distribution of Ez over
                    %-1 < y < 1, where the radius of the cavity is set to 1.
                if sqrt(x^2 + y^2) <= 1 % Only calculate something if (x,y) falls within
                            %a circle of radius 1
                    EHstructure = cavResFunction(sqrt(x^2 + y^2),...
                        atan2(y,x),pos,modeString); % Calculate the actual value of E_mag
                                            %at the specific (x,y)
```

```matlab
                E_mag(k,l) = EHstructure.E_mag;
            end
            l = l + 1; % Update the index variables
        end
        k = k + 1; % Update the index variables
    end
    delete(waitH) % Close/delete the waitbar

    % Construct a surface over -1 < x,y < 1 at z = pos
    x = [-1 1];
    y = [-1 1];
    z = pos*ones(2,2);

    % Create a truecolor (RGB) plane of surfColor color
    % with the same size as Ez
    EPlane(:,:,1) = surfColor(1)*ones(size(E_mag));
    EPlane(:,:,2) = surfColor(2)*ones(size(E_mag));
    EPlane(:,:,3) = surfColor(3)*ones(size(E_mag));

    % Create a plane serving as transparancy (alpha) channel for
    % the colored plane. Its value is associated with the value of E_mag:
    % If E_mag is maximum the plane should be opaque, if E_mag = 0 it should
    % be fully transparent.
    alphaPlane = uint8(255*E_mag'/E_max);

    % Create the actual Matlab surface using the colored plane
    % and its alpha channel (see Matlab docs for more
    % information about surface and its properties)
    h = surface(x,y,z,EPlane,'FaceColor','texturemap',...
        'EdgeColor',borderColor,'LineWidth',edgeWidth,...
        'CDataMapping','direct',...
        'AlphaData',alphaPlane,'FaceAlpha','texturemap');

case 'x' % A yz-plane at constant x. The mechanics are pretty similar to the
    %z-plane, so comments have been omitted.
    E_mag = zeros(steps,steps);
    x = pos;

    k = 1;
    waitH = waitbar(0,'Running...');
    for y = linspace(-1,1,steps)
        mess = sprintf('Running... (%d/%d)',k,steps);
        waitbar((k-1)/steps,waitH,mess)
        l = 1;
        for z = linspace(0,1,steps)
            if sqrt(x^2 + y^2) <= 1
                EHstructure = cavResFunction(sqrt(x^2 + y^2),...
                    atan2(y,x),z,modeString);
                E_mag(k,l) = EHstructure.E_mag;
            end
            l = l + 1;
        end
        k = k + 1;
    end
    delete(waitH)

    x = [pos pos; pos pos];
    y = [-1 -1; 1 1];
    z = [0 1; 0 1];

    EPlane(:,:,1) = surfColor(1)*ones(size(E_mag));
    EPlane(:,:,2) = surfColor(2)*ones(size(E_mag));
    EPlane(:,:,3) = surfColor(3)*ones(size(E_mag));

    alphaPlane = uint8(255*E_mag/E_max);

    h = surface(x,y,z,EPlane,'FaceColor','texturemap',...
        'EdgeColor',borderColor,'LineWidth',edgeWidth,...
        'CDataMapping','direct',...
        'AlphaData',alphaPlane,'FaceAlpha','texturemap');
case 'y' % An xz-plane at constant x. The mechanics are pretty similar to the z-plane,
    %so comments have been omitted.
    E_mag = zeros(steps,steps);
```

```matlab
        y = pos;

        k = 1;
        waitH = waitbar(0,'Running...');
        for x = linspace(-1,1,steps)
            mess = sprintf('Running... (%d/%d)',k,steps);
            waitbar((k-1)/steps,waitH,mess);
            l = 1;
            for z = linspace(0,1,steps)
                if sqrt(x^2 + y^2) <= 1
                    EHstructure = cavResFunction(sqrt(x^2 + y^2),...
                        atan2(y,x),z,modeString);
                    E_mag(k,l) = EHstructure.E_mag;
                end
                l = l + 1;
            end
            k = k + 1;
        end
        delete(waitH)

        y = [pos pos; pos pos];
        x = [-1 -1; 1 1];
        z = [0 1; 0 1];

        EPlane(:,:,1) = surfColor(1)*ones(size(E_mag));
        EPlane(:,:,2) = surfColor(2)*ones(size(E_mag));
        EPlane(:,:,3) = surfColor(3)*ones(size(E_mag));

        alphaPlane = uint8(255*E_mag/E_max);

        h = surface(x,y,z,EPlane,'FaceColor','texturemap',...
            'EdgeColor',borderColor,'LineWidth',edgeWidth,...
            'CDataMapping','direct',...
            'AlphaData',alphaPlane,'FaceAlpha','texturemap');

    case 'angle'
        E_mag = zeros(steps,steps);

        k = 1;
        waitH = waitbar(0,'Running...');
        for r = linspace(-1,1,steps)
            mess = sprintf('Running... (%d/%d)',k,steps);
            waitbar((k-1)/steps,waitH,mess)
            l = 1;
            for z = linspace(0,1,steps)
                    EHstructure = cavResFunction(r,pi/2-pos*pi/180,z,modeString);
                    E_mag(k,l) = EHstructure.E_mag;
                l = l + 1;
            end
            k = k + 1;
        end
        delete(waitH)

        x = [sind(pos) sind(pos); -sind(pos) -sind(pos)];
        y = [cosd(pos) cosd(pos); -cosd(pos) -cosd(pos)];
        z = [1 0; 1 0];

        EPlane(:,:,1) = surfColor(1)*ones(size(E_mag));
        EPlane(:,:,2) = surfColor(2)*ones(size(E_mag));
        EPlane(:,:,3) = surfColor(3)*ones(size(E_mag));

        alphaPlane = uint8(255*E_mag/E_max);

        h = surface(x,y,z,EPlane,'FaceColor','texturemap',...
            'EdgeColor',borderColor,'LineWidth',edgeWidth,...
            'CDataMapping','direct',...
            'AlphaData',alphaPlane,'FaceAlpha','texturemap');
end
```

Appendix B

Simulating the one dimensional electric field profile using Matlab

This script has a lot in common with the script described in appendix A. The difference is the finite size of the PVC cube. In this script, the dielectric dimensions can be put in together with the position (height) of the dieletric. Together with the mode (modeStr) and the number of elements per coordinate (numEl, which is a size for the amount of discretization steps) the script calculates the electric field of a certain mode taking into account the finite size of the PVC cube. The script uses a loop to move the PVC cube along the cavity, at each point calculating the local electric field. This way a figure like figure 4.8 on page 19 can be constructed.

The script makes use of a function named cavResFunction, which calculates the electric field from equation (2.7).

```matlab
% Input parameters
 % Mode
 modeStr = 'TM412';

 % Number of elements per coordinate (total size of array numEl^3)
 numEl = 20;

 % Dimensions dielectric
 xd = 10/87.5; % Normalized w.r.t. radius
 yd = 10/87.5; % Normalized w.r.t. radius
 zd = 1/65; % Normalized w.r.t. height

 % Position dielectric
 rho = linspace(0,1,100); % Normalized w.r.t. radius
 phi = deg2rad(0); % In radians
 z = .7; % Normalized w.r.t. height

% Body
 % Integration box
 for k = 1:length(rho);
     clear E_sq;

     % Cylindrical -> Cartesian
     rhoCurr = rho(k);
     phiCurr = phi;
     zCurr = z;
     [xCurr,yCurr] = pol2cart(phiCurr,rhoCurr);

     [X,Y,Z] = meshgrid(linspace(xCurr-xd,xCurr+xd,numEl),...
         linspace(yCurr-yd,yCurr+yd,numEl),...
         linspace(zCurr-zd,zCurr+zd,numEl));

     % Cartesian -> cylindrical
     [PHI,RHO] = cart2pol(X,Y,Z);
     E_struct = cavResFunction(RHO,PHI,Z,modeStr);
     E_sq = E_struct.E_mag.^2;
```

```
    E_out(k) = nansum(nansum(nansum(E_sq)));
end
E_out = E_out./max(E_out);
rho = 10*rho;
figure;plot([fliplr(-rho) rho],[fliplr(E_out) E_out],':o')
```

```
E_out = E_out./max(E_out);
rho = 10*rho;
figure;plot([fliplr(-rho) rho],[fliplr(E_out) E_out],':o')
```

Appendix C

Canny edge void detection using Matlab

This Matlab script is used to detect the edges of the void and thus determine the void size. It is used for figure 4.16.

```matlab
clear % Be careful not to erase important stuff in your workspace!

% Configuration
inputFolder = 'Input folder here'; % Directory with grayscale images
outputFolder = 'Input folder here'; % Directory to output the overlay pictures and MAT-file
writeMat = true; % Save a MAT-file with voidCrossSection etc. to the output directory
testMode = 3;    % The script can output the progress to a figure window. Options:
                 % 1: ROI with BW contours and void
                 % 2: CData with void overlay
                 % 3: Plot voidCrossSection
                 % Other: No plots whatsoever

frameRange = 500:2400; % Frame range for which void analysis should be carried out. This can also be
% one frame of course
frameRegionHeight = 195:595; % Vertical region of interest (ROI) in pixel indices.
frameRegionWidth = 60:940; % Horizontal ROI in pixel indices.
xCentre = 454; % Horizontal position of the void centre in pixels w.r.t. the left edge of the ROI
yCentre = 60; % Vertical position of the void centre in pixels w.r.t. the top edge of the ROI
edgeThresh = [.15 .35]; % Threshold array (2 elements) for Canny edge detection
edgeSigma = 6; % Sigma (Gaussian blur radius) for Canny edge detection
% ---
edgeThresh = repmat(edgeThresh,[frameRange(end) 1]);
edgeSigma = repmat(edgeSigma,[frameRange(end) 1]);
% ---
    % Per-frame correction for Canny edge detection, e.g. for frame 100
    % edgeThresh(100) = [a b];
    % edgeSigma(100) = c;
    edgeSigma([824 831 838 842 848 858 861 874 876 885 892 909 936 1121 1255 1266 1272 1284
        1707 1736 1737 1741 1754 1775 1788 2111 2121 2150]) = 6.9;
    edgeSigma(885) = 6.8;

% Memory allocation
voidCrossSection = NaN*ones(frameRange(end),1);
voidSurfaceArea = NaN*ones(frameRange(end),1);
voidVolume = NaN*ones(frameRange(end),1);
xyData(frameRange(end)).X = [];
xyData(frameRange(end)).Y = [];

% Main
warning('off','images:imshow:magnificationMustBeFitForDockedFigure') % Suppress annoying warnings for
% imshow combined with a docked figure
system(['mkdir "' outputFolder '"']); % Create the output directory
for k = frameRange % Loop over the selected frames
    if isequal(rem(k,100),0) % Output the frame number every 100 frames
        fprintf('%d\n',k)
    end
```

```matlab
imFile = fullfile(inputFolder,sprintf('frame%05d.png',k)); % Combine the directory and filename
    %into a complete (Windows) path
cdata = imread(imFile); % Read the grayscale data into an imHeight x imWidth array
cdataOrig = cdata; % Copy the original image array to a back-up variable

% Select the ROI
cdata = cdata(frameRegionHeight,frameRegionWidth);

% Carry out Canny edge detection. BW is a binary image containing the
% detected edges
[BW, thresh] = edge(cdata,'canny',edgeThresh(k,:),edgeSigma(k));

% Search pixels closest to void centre
conn = bwconncomp(BW); % Find connected pixels in the edge-detected image

yOld = []; yOldTop = [];xVoid = [];yVoid = [];xVoidTop = []; yVoidTop = [];
for n = 1:conn.NumObjects % Loop over all the connected curves
    pixList = conn.PixelIdxList;
    pixLin = pixList{n};
    [Y,X] = ind2sub(size(cdata),pixLin); % x and y coordinates of the curve
    voidIdx = find(X == xCentre); % Look for a curve with x = yCentre
    if ~isempty(voidIdx)
        yCurr = Y(voidIdx);
        yCurr = yCurr(yCurr > yCentre); % Find a curve that lies below yCentre
        if length(yCurr) > 1
            yCurr = yCurr(1);
        end
        if ~isempty(yCurr) % Find the one closest to yCentre
            if isempty(yOld)
                yOld = yCurr;
                xVoid = X;
                yVoid = Y;
            elseif yCurr < yOld
                yOld = yCurr;
                xVoid = X;
                yVoid = Y;
            end
        end
        yCurrTop = Y(voidIdx);
        yCurrTop = yCurrTop(yCurrTop < yCentre); % Find a curve that lies above yCentre
        if length(yCurrTop) > 1
            yCurrTop = yCurrTop(1);
        end
        if ~isempty(yCurrTop) % Find the one closest to yCentre
            if isempty(yOldTop)
                yOldTop = yCurrTop;
                xVoidTop = X;
                yVoidTop = Y;
            elseif yCurrTop > yOldTop
                yOldTop = yCurrTop;
                xVoidTop = X;
                yVoidTop = Y;
            end
        end
    end
end

% Discard the void wings
    % Left
idx = xVoid < xCentre;
yLeft = yVoid(idx);
xLeft = xVoid(idx);
id = yLeft < yCentre;
xTop = xLeft(id);
yTop = yLeft(id);
idxLeft = find(idx);
idxLeft = idxLeft(id);

xCurr = 0;
X = [];
Y = [];
for y = yCentre:-1:1
    xFound = xTop(yTop == y);
```

```matlab
        xFound = max(xFound);
        if xFound > xCurr
            X = [X xFound];
            Y = [Y y];
            xCurr = xFound;
        end
end
xLeft = X;
yLeft = Y;

    % Right
idx = xVoid > xCentre;
yRight = yVoid(idx);
xRight = xVoid(idx);
id = yRight < yCentre;
xTop = xRight(id);
yTop = yRight(id);
idxRight = find(idx);
idxRight = idxRight(id);

xCurr = Inf;
X = [];
Y = [];
for y = yCentre:-1:1
    xFound = xTop(yTop == y);
    xFound = min(xFound);
    if xFound < xCurr
        X = [X xFound];
        Y = [Y y];
        xCurr = xFound;
    end
end
xRight = X;
yRight = Y;

    % Merge
yVoid([idxLeft; idxRight]) = [];
xVoid([idxLeft; idxRight]) = [];
xVoid = [xLeft xVoid' xRight];
yVoid = [yLeft yVoid' yRight];
%----

% Merge top and bottom
if ~isempty(xVoidTop) && ~isempty(xVoid)
    xMin = min(xVoid);
    xMax = max(xVoid);
    idx = xVoidTop > xMin & xVoidTop < xMax;
    xVoidTop = xVoidTop(idx);
    yVoidTop = yVoidTop(idx);
    X = [xVoidTop' xVoid];
    Y = [yVoidTop' yVoid];
else
    X = xVoid;
    Y = yVoid;
end

% Sort x,y-pairs with increasing angle
[theta,rho] = cart2pol(xCentre-X,Y-yCentre);
idx = theta < 0 & theta < -pi/2;
theta(idx) = theta(idx) + 2*pi;
[theta,idx] = sort(theta);
rho = rho(idx);
[X,Y] = pol2cart(theta, rho);
X = xCentre-X;
Y = Y+yCentre;

% Extrapolation of void to top of frame
if isempty(xVoidTop) && ~isempty(X)
    if Y(1) ~= 1
        Y = [1 Y];
        X = [X(1) X];
    end
    if Y(end) ~= 1
```

```matlab
            Y = [Y 1];
            X = [X X(end)];
        end
    end

    % Calculation of voidCrossSection, etc.
    if length(unique(X)) > 1
        geom = polygeom(X,Y); % Calculate the are, centroids and perimeter of the polygon
        voidCrossSection(k) = geom(1);

        % Void volume and surface area
        idx = X <= xCentre;
        xLeft = X(idx);
        yLeft = Y(idx);
        xRight = X(~idx);
        yRight = Y(~idx);

        if length(unique(xLeft)) > 1 && length(unique(xRight)) > 1
            % Left half
            if Y(1) == 1 && Y(end) == 1
                halfGeom = polygeom(xLeft,yLeft);
                arcLength = halfGeom(4);

                xLeft = [xCentre xLeft];
                yLeft = [1 yLeft];
                halfGeom = polygeom(xLeft,yLeft);
                xCentroid = xCentre - halfGeom(2);
            else
                halfGeom = polygeom(xLeft,yLeft);
                xCentroid = xCentre - halfGeom(2);
                arcLength = halfGeom(4);
            end
            voidVolumeLeft = 2*pi*xCentroid*halfGeom(1);
            voidSurfaceAreaLeft = 2*pi*xCentroid*arcLength;

            % Right half
            if Y(1) == 1 && Y(end) == 1
                halfGeom = polygeom(xRight,yRight);
                arcLength = halfGeom(4);

                xRight = [xRight xCentre];
                yRight = [yRight 1];
                halfGeom = polygeom(xRight,yRight);
                xCentroid = halfGeom(2) - xCentre;
            else
                halfGeom = polygeom(xRight,yRight);
                xCentroid = halfGeom(2) - xCentre;
                arcLength = halfGeom(4);
            end
            voidVolumeRight = 2*pi*xCentroid*halfGeom(1);
            voidSurfaceAreaRight = 2*pi*xCentroid*arcLength;

            voidVolume(k) = mean([voidVolumeLeft voidVolumeRight]);
            voidSurfaceArea(k) = mean([voidSurfaceAreaLeft voidSurfaceAreaRight]);
        else
            voidCrossSection(k) = NaN;
            voidVolume(k) = NaN;
            voidSurfaceArea(k) = NaN;
        end
    else
        voidCrossSection(k) = NaN;
    end

cmap = gray(256); % The usual 8-bit grayscale color map
if ~isempty(find(BW,1));
    cdata(BW) = 256; % Color the detected edges white
end

if ~isempty(X)
    voidMask = poly2mask(X+frameRegionWidth(1)-1,Y+frameRegionHeight(1)-1,...
        size(cdataOrig,1),size(cdataOrig,2)); % Create a mask where the void is detected

    cdataOrig = ind2rgb(cdataOrig,cmap); % Convert the original grayscale image to RGB color space
```

```matlab
        overlayColor = [1 0 0]; % The overlay color for the void is red
        edgeColor = [0 1 1]; % The color to give the edges is cyan (green + blue)
        cdataC = zeros(size(cdataOrig(:,:,1)));
        cdataVoid = zeros(size(cdataOrig));
        for n = 1:3
            cdataC = cdataOrig(:,:,n);
            cdataC(voidMask) = imadd(cdataOrig(voidMask),.5*overlayColor(n));
            cdataEdge = cdataC(frameRegionHeight,frameRegionWidth);
%             cdataEdge(BW) = edgeColor(n);
            cdataVoid(:,:,n) = cdataC;
            cdataVoid(frameRegionHeight,frameRegionWidth,n) = cdataEdge;
        end
        cdataVoid(yCentre+frameRegionHeight(1)-1,xCentre+frameRegionWidth(1)-1,:) = [0 1 0];
    else
        cdataVoid = ind2rgb(cdataOrig,cmap);
    end

    switch testMode
        case 1
%             set(gcf,'WindowStyle','normal')
            imshow(cdata,[],'InitialMagnification',100)
            hold on
            plot(xCentre,yCentre,'xc')
            plot(X,Y,'.g')
            hold off
            title(sprintf('%d',k))
            drawnow
        case 2
            set(gcf,'WindowStyle','normal')
            imshow(cdataVoid,'Initialmagnification',100)
            hold on
            plot(X+frameRegionWidth(1)-1,Y+frameRegionHeight(1)-1,'xg')
            hold off
            title(sprintf('%d',k))
            drawnow
        case 3
            plot(voidCrossSection,'.')
            drawnow
    end

    imwrite(cdataVoid,...
        fullfile(outputFolder,sprintf('void%05d.png',k)),'png')

    Xreal = X+frameRegionWidth(1)-1;
    Yreal = Y+frameRegionHeight(1)-1;
    xyData(k).X = Xreal;
    xyData(k).Y = Yreal;
end

if writeMat
    save([outputFolder '\voidAnalData.mat'],...
        'voidCrossSection','voidSurfaceArea','voidVolume',...
        'xCentre','yCentre',...
        'xyData','frameRange','-v7.3')
end
```